COLLEGE OF BASIC AND APPLIED SCIENCES

SCHOOL OF PHYSICAL AND MATHEMATICAL SCIENCES

UNIVERSITY OF GHANA

PETROGRAPHY AND GEOCHEMISTRY OF SCHISTS AND AMPHIBOLITES FROM THE PALEOPROTEROZOIC BIRIMIAN SUHUM BASIN, SOUTHEASTERN GHANA.

PRESENTED

By

ADIAMAH SUSSUANA SEYRAM

(10272783)

A THESIS SUBMITTED TO THE UNIVERSITY OF GHANA, LEGON IN PARTIAL FULFILLMENT OF THE REQUIREMENTS FOR THE AWARD OF A MASTER OF PHILOSOPHY DEGREE IN GEOLOGY

JULY, 2016.

DECLARATION

I, Sussuana Seyram Adiamah, declare that this work is original and done by me under the supervision of Professor Daniel K. Asiedu and Dr. Chris Y. Anani. This work has not been submitted for other qualifications either in whole or in part in any institution. All supporting literature used have been duly referenced.

…….. Date……

ADIAMAH SUSSUANA SEYRAM

(Student)

……..... Date…….

PROF. D.K. ASIEDU

(Principal Supervisor)

…… Date…….

DR. CHRIS ANANI

(Co-Supervisor)

ABSTRACT

The mineralogical composition; as well as, major and trace-element geochemistry of the schists and amphibolites from the northwestern portion of the Suhum basin, were studied to determine the provenance, petrogenesis and tectonic implications of the Basin in relation to the surrounding Birimian rocks.

Thirty (30) thin sections were prepared for petrographical studies. Twenty-five (25) samples were analysed for their major and trace elements contents. From the petrography, the rocks are composed of biotite schists, hornblende-biotite schists, muscovite-biotite schists and amphibolites.

The hornblende-biotite schists and muscovite biotite schists are metasedimentary in nature. From the major and trace element analysis, however, the schists are classified as greywackes (Fe-shales and wackes) whiles the amphibolites classified as para-amphibolites and ortho-amphibolites. The source rocks of the schists have undergone incipient to intermediate degrees of weathering and low degrees of sediment reworking (recycling). The schists are texturally and mineralogically immature and were derived from mafic to felsic rock sources; possibly from the lower crustal to upper mantle regions.

Petrographical and geochemical characteristics suggest the deposition of the schists probably within active continental margin and arc margin settings. Provenance indicators suggest mafic, intermediate and felsic igneous provenances for the schists.

Taken together, the overall inferred provenance of the schists could be that of Young Undifferentiated Arc terranes (YUA). Hence, the source area for the sediments of the schists is most likely the adjacent Birimian metavolcanic rocks.

The amphibolites from the study area are classified as metaluminous, gabbroic and subalkaline (tholeiitic). Both para-amphibolites and ortho-amphibolites were identified to have been derived from zones typically characteristic of Mid-Ocean Ridge Basalts (MORBs), Island Arc Tholeiites (IATs) and Continental Arc Basalts (CABs).

The amphibolites were most probably derived from the adjacent Birimian granite-greenstone belts and show characteristics similar to the Archean greenstone belts. This supports the fact that the Paleoproterozoic terranes of the West African Craton resemble the Archean greenstone terranes.

DEDICATION

This work is dedicated to the Almighty God, the Adiamah, Agbo, Owusu and Boateng families.

ACKNOWLEDGEMENTS

"All the victory belongs to Jesus Christ."

I am forever grateful to God for His grace, mercy and favour, which enabled me successfully complete this thesis. I could never have made it without His mighty hand over me.

I would like to express my deepest gratitude to my supervisors; Prof. Daniel K. Asiedu and Dr. Chris Y. Anani for their exceptional guidance, support, encouragement, as well as, academic and technical input. I am also grateful to Dr. Solomon Anum for his assistance in this research.

I would like to appreciate my family for their love, support and encouragement. I am especially grateful to Mr. Edwin Adiamah, Mrs. Nellie Agbo, Mr. and Mrs. Owusu and Nana Owusu Boateng for believing in me.

I am highly indebted to the Department of Earth Science Capacity Building Project, University of Ghana, Legon, for financially supporting me throughout the pursuance of my degree.

Finally, my heartfelt appreciation goes to Prof. P.M. Nude for all his support and encouragement. To Mr. Daniel Kwayisi, I would like to say a very big thank you for your vigorous training which has shaped me up. I would like to acknowledge Mrs. Naa Afi Agrah and Ms. Abigail Ayikwei whose love, support and encouragement, have helped me in so many ways.

TABLE OF CONTENTS

LIST OF FIGURES

LIST OF TABLES

CHAPTER ONE

INTRODUCTION

1.1. BACKGROUND

The West African Craton (W.A.C.), is composed of Archean and Paleoproterozoic (Birimian) rocks in areas which have been identified to represent a major zone of crustal growth (Abouchami et al., 1990; Boher et al., 1992; Taylor et al., 1992). The Paleoproterozoic Birimian Supergroup according to Junner (1940), is found at the north and east of the Leo-Man shield, occupying the southern part of the West African Craton in Figure 1.1.

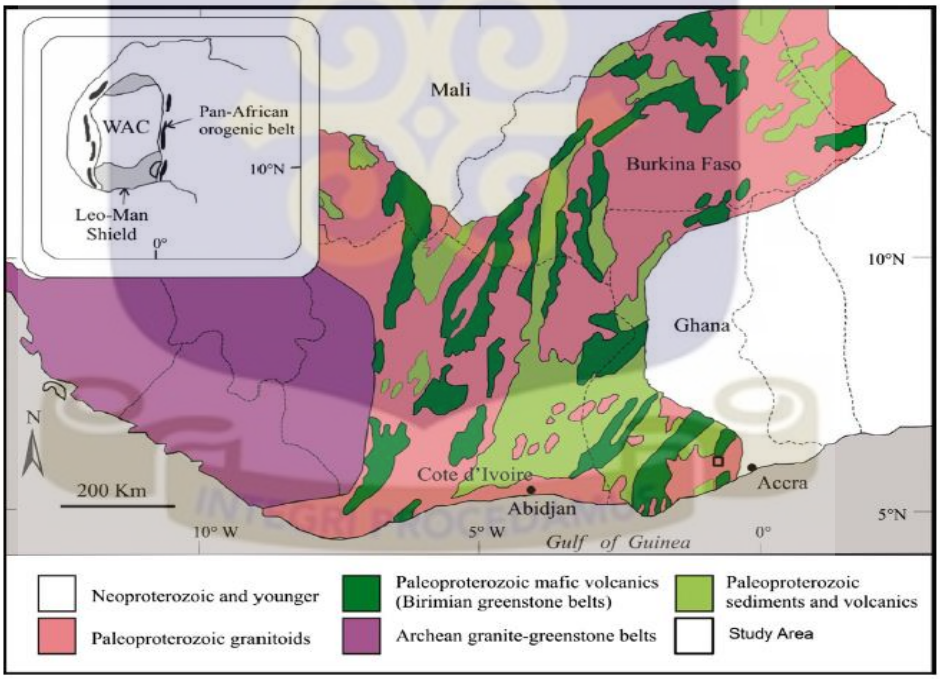

Figure 1.1 Simplified geological map of the Man shield showing the rocks of the three different eras; inset showing the West African Craton separating the Reguibat and Leo-Man Shields, as well as the Pan-African Orogenic belt (Modified after Attoh et al., 2006).

The Birimian Supergroup is a new crust formed at a time of dormancy in the North American-Europe regions and Australia. It comprises units (Abouchami et al., 1990) of;

1. Volcano-detrital rocks
2. Bimodal and tholeiitic volcanics.

It is host to a number of economic minerals, and has received a lot of attention with respect to research and exploration activities from geoscientist for nearly a century.

According to Leube et al. (1990), these Birimian rocks have undergone deformation, regional metamorphism and were tectonically stable during the Eburnean orogeny (ca. 2000 Ma). The Leo-Man shield, comprises of Liberian aged Archean rocks (3.0-3.5 Ga) to the west and the early Proterozoic Birimian Supergroup to the east (Leube et al., 1990).

All the attention received by the Birimian rocks over the years, have resulted in contradictory interpretations about the geodynamic model of the Birimian Paleoproterozoic rocks. Researchers like Leube et al. (1990), have proposed various accretionary models for the evolution of the Birimian series and the Eburnean orogeny. Numerous conclusions including the intraplate oceanic plateau settings by Abouchami et al. (1990); intracratonic rift to oceanic-spreading; immature island arcs built on oceanic crust according to Sylvester and Attoh (1992) and, a back-arc basin by Vidal and Alric (1994) were made from all the research work done.

In Ghana, six main Paleoproterozoic Birimian granite-greenstone belts and their intervening metasedimentary basins have been identified. These granite-greenstone belts include the Kibi-Winneba belt, the Ashanti belt, the Sefwi-Bibiani belt, the Bui belt, the Bole-Nangodi belt and the Lawra belt. All the various granite-greenstone belts except the Lawra belt, trend NE-SW (Griffis et al., 2002). Their intervening metasedimentary basins include the Maluwe basin, Cape Coast basin, Kumasi basin, Suhum basin and Sunyani basin (Figure 1.2).

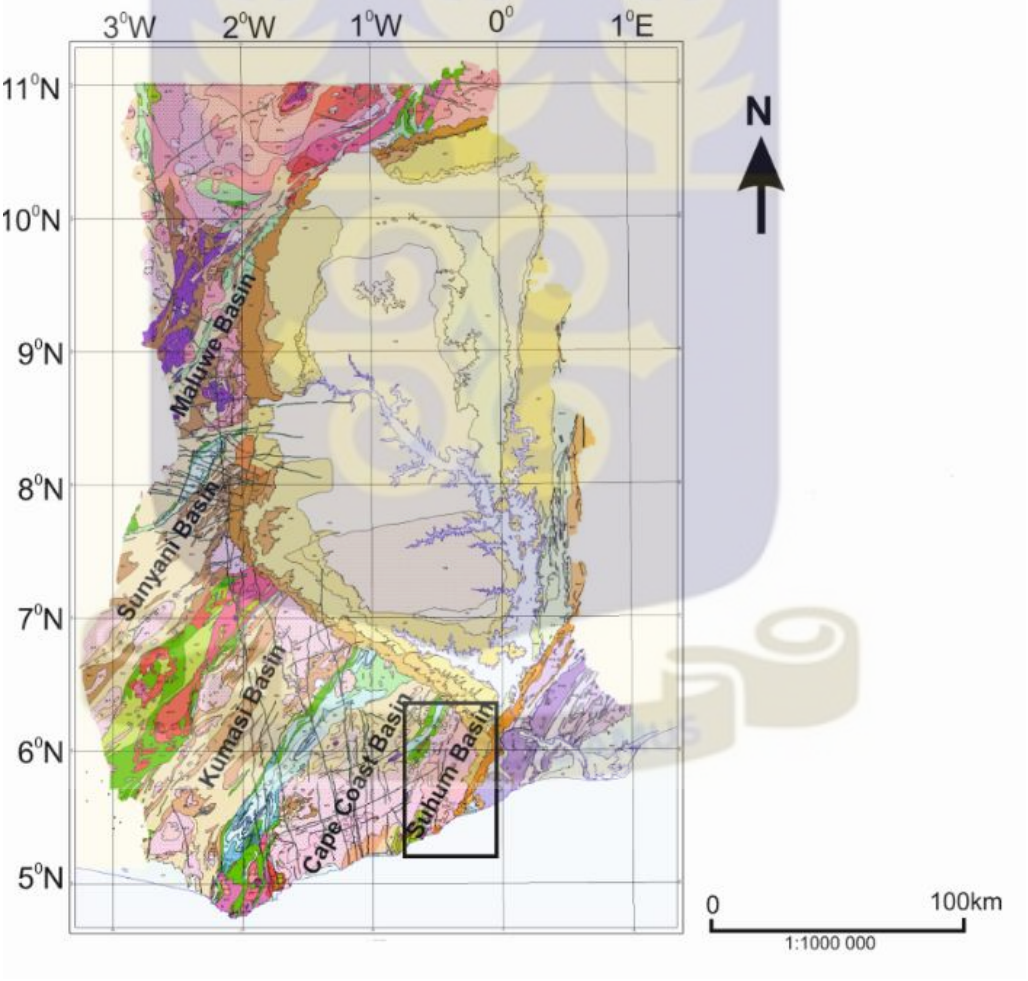

Figure 1.2 Geological map of Ghana showing the various intervening metasedimentary basins; inset showing the Birimian Paleoproterozoic Suhum Basin, southeastern Ghana (modified after the Ghana National Geological Map Project; 2009).

The Birimian metasedimentary basins in Ghana are filled with volcaniclastic rocks, wackes and argillites, intruded by aluminous granitic plutons (Leube et al., 1990). The metavolcanic belts, on the other hand, are made up of meta-tholeiitic lavas, minor volcaniclastics as well as "belt-type" granitoids. The basins have undergone amphibolite facies metamorphism whereas the belts, greenschist facies metamorphism. (Leube et al., 1990; Sylvester and Attoh., 1992).

Geochronological studies conducted by researchers like Liégeois et al. (1991); Boher et al. (1992), Hirdes et al. (1992); and Davis et al. (1994), on the West African Birimian Supergroup and associated granitoids, suggest rock ages dating back to ~2.25-2.05 Ga. Hence, the rocks were probably deposited on an Archean basement as sediments and volcanics in the early Proterozoic, and later deformed during the Eburnean tectono-thermal event.

Of all the six main Paleoproterozoic Birimian granite-greenstone belts and their intervening metasedimentary basins in Ghana, the Suhum basin (Figure 1.2), situated at the eastern portion of the Cape Coast basin has received very little attention in terms of petrographic and geochemical studies.

The general geology as well as the petrogenesis, provenance and tectonic settings of the rocks within this basin have not been extensively documented. It is therefore necessary to gather as much petrological and geochemical data from areas covered by the Suhum Basin rocks to draw important conclusions on the petrogenesis, provenance, and tectonic implications of the basin in relation to surrounding Birimian rocks. The purpose of this study is to report the petrographic and geochemical compositions of the rocks within the Paleoproterozoic Birimian Suhum Basin, southeastern Ghana.

1.2. AIM

To determine the petrographical and geochemical characteristics of the schists and amphibolites within the Paleoproterozoic Birimian Suhum basin to infer the probable petrogenesis, provenance and tectonic settings within which they formed.

1.3. OBJECTIVES

The objectives of this study is to: -

1. Characterize the mineral and geochemical composition of the rocks within the study area.
2. Identify the various rock types within the study area.
3. Constrain the petrogenesis, provenance and tectonic settings of these rocks.
4. Examine the post-depositional compositional changes affecting these rocks.
5. Provide information on the paleo-weathering conditions at the source area(s).
6. Compare the findings of this study to findings from research conducted on other Basins to determine the existence of similarities and/ differences in their individual geologic histories.

1.4. SCOPE

This study is focused on the schists and amphibolites of the Birimian Supergroup and integrates petrography and geochemistry in studying the petrogenesis, provenance and tectonic settings of some rock formations of the Birimian, to aid in a better understanding of the geologic history of the Birimian Supergroup. Samples were collected from the area under investigation to achieve this aim.

1.5. STUDY AREA

1.5.1. Location and accessibility

The study area is located within the Eastern Region of Ghana and consists of selected areas in the Adeiso, Ayensuano and Asamankese districts. These areas include towns such as Dorkrokyewa, Kyenkulabi, Oparekurom, Obudanfo, Yawapem, Duodokurom, Kwamekyerekurom, Amfaso, Akwatikurom and Kofiansah (Figure 1.3).

An approximate area of 215 km^2 was covered within latitudes 6°00'00"N and 5°50'00"N; and longitudes 0°33'00"E and 0°27'00"E. Dorkrokyewa, one of the major towns within the area provided a suitable linkage as well as a point of referencing to all the other areas studied. The study area can mainly be accessed through second and third class roads. These roads, however, adjoin a major road which cuts through the north-western portion of the area. Towns such as those en route Yawapem through Dorkrokyewa, Coaltar and Amfaso can be accessed by a first class road. From Sowate to Kyenkulabi, Coaltar, Bepowase through to Aidokofi can be accessed by third class roads. There are also footpaths, forming networks connecting roads and farms to the outcrops observed. The road network within the study area is in a relatively good shape; and evidence of ongoing road construction projects show possible improvements in the near future.

The study area is covered mostly by Birimian Paleoproterozoic rocks. Dickson and Benneh (1988), noted agriculture as the main source of livelihood for majority of the inhabitants in the area.

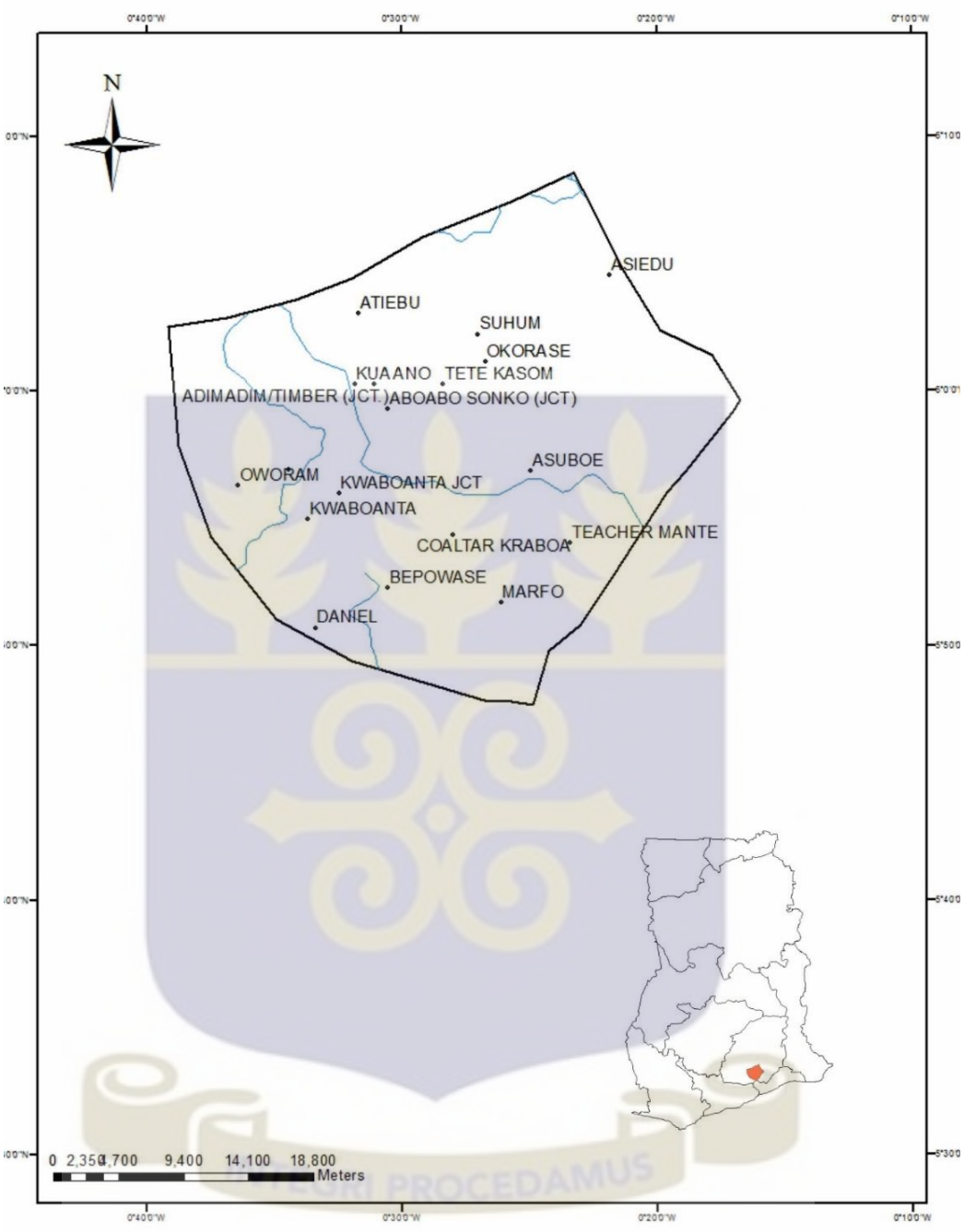

Figure 1.3. A map of the study area showing the towns within the three districts in the Eastern Region of Ghana; orange portion of the map of Ghana showing location of study area.

1.5.2. Topography and drainage

According to Dickson and Benneh (1988), the topography of the study area is generally hilly and undulating with a few flat areas. Steep low hills and ridges usually break up the topography in several places. These hills are scattered almost throughout the topographic map. The central and southwestern portions of the study area are relatively higher with heights ranging between 350 ft-1050 ft above sea level.

The study area is well drained and networked by a dendritic pattern of rivers, which often take their source from the hills and mountain ranges flowing downhill through the area. The others are mostly tributaries to larger perennial rivers. During the rainy seasons, those perennial rivers swell up; flooding over large areas. However, the tributaries of those rivers are often reduced or do not flow at all during the main dry season. The major perennial rivers flow approximately to the regional strike resulting in the dendritic pattern.

1.5.3. Geological setting

In Ghana, the Birimian is characterized by sedimentary basins, which separate a series of sub-parallel, roughly spaced, north-easterly-trending volcanic belts. The study area lies within the Suhum basin; its geology has however not been studied extensively. From Figure 1.4, the basin is surrounded by the Cape Coast basin on the left and the Voltaian Supergroup and Buem units to the right.

The major underlying rock formation within the study area is the Birimian. The rocks of the Birimian Supergroup are economically the most important geological formation in Ghana; since it hosts most of the valuable minerals exported for foreign exchange

such as gold, bauxite and diamonds. Gold is believed to be in some of the districts within the study area but is currently unexploited.

Geologically, the area under study was covered by Birimian Paleoproterozoic rocks such as mica-schists, metavolcanic rocks, amphibolites, pegmatites and gneisses. The schists being the main focus of the study to occur in the following under listed forms on the field;

1. As outcrops on their own; as was observed in the river flowing through Oparekurom (N 05°57'20.0" and W 000°31'22.5").
2. Alongside the pegmatites; observed at the various road cuts within the study area.

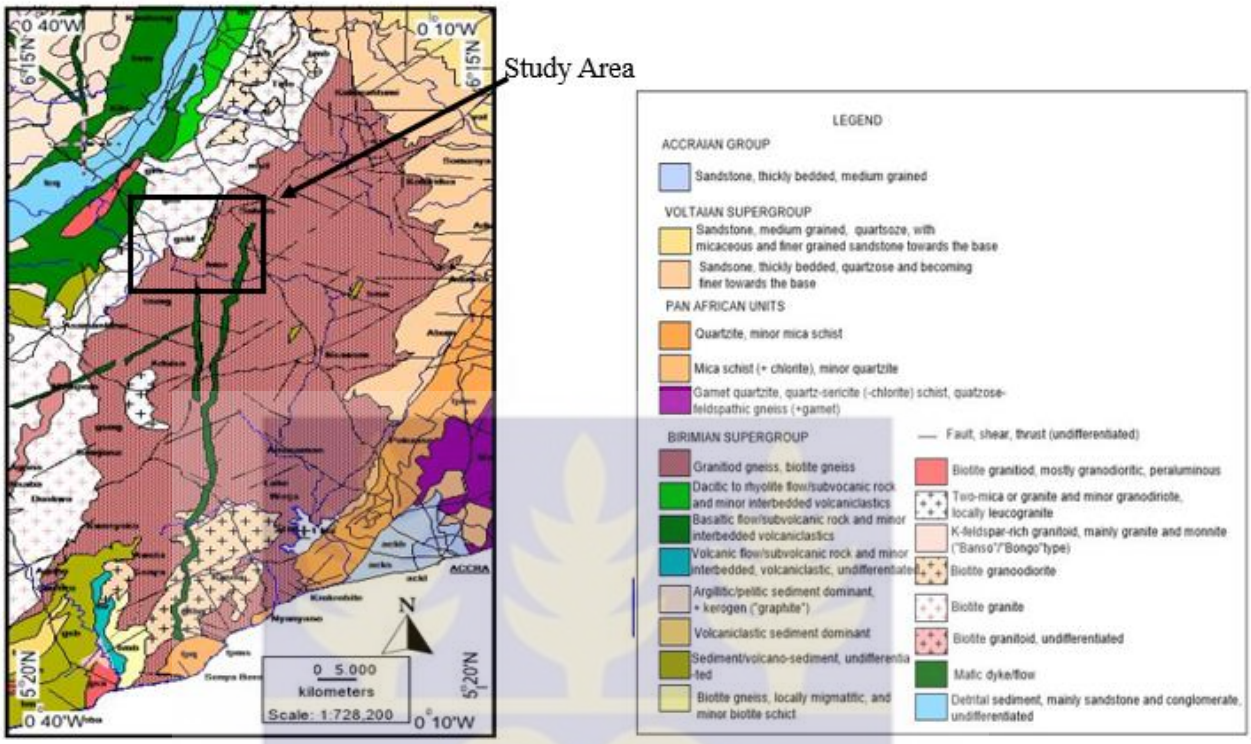

Figure 1.4 A geological map of the study area located at the northwestern portion of the Suhum basin, south-eastern Ghana; Inset shows the study area (map extracted from the Geological Map of Ghana Project; 2009).

CHAPTER TWO

LITERATURE REVIEW

2.1. THE WEST AFRICAN CRATON

The West African Craton (W.A.C.) is a large mass, or craton, of Precambrian basement rocks constituting the African Plate. This craton according to Ennih and Liégeois (2008), has been stable since 2 Ga after it had been affected by the Eburnean Orogeny. It is made up of three Archean and Paleoproterozoic metamorphic and magmatic shields: the Leo-Man Shield, the Anti-Atlas and Reguibat Shield, separated by two cratonic sedimentary basins.

The geological framework of the West African Craton (Figure 2.1), is made up of the Man shield to the south, to which Kayes and Kenieba Inliers are associated; the Reguibat shield to the north; and further north is the Anti-Atlas Belt. Between the two shields are the Tindouf and Neoproterozoic to Paleozoic Taoudeni basins.

The basement of the West African Craton was built through numerous major orogenic cycles; the Paleoarchean-Leonian cycle (multiple events between 3.5 and 3.0 Ga) related to continental accretion and volcano-sedimentary activity with an uncertain chronology; the 2.95-2.75 Ga Liberian cycle, the 2.2-1.75 Ga Eburnean-Birimian cycle and the recent 760-660 Ma Pan-African orogenic event (Thiéblemont et al., 2004).

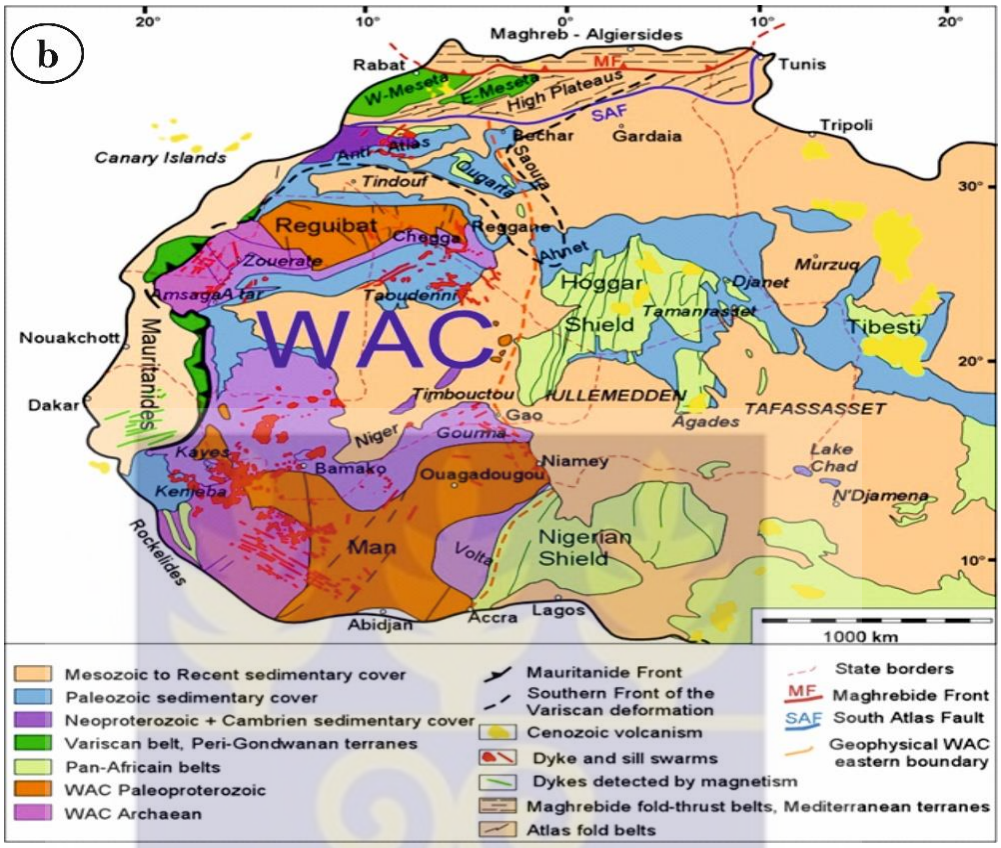

Figure 2.1 Map of the general geology of the West African Craton (Fabre, 2005; Liégeois et al., 2005; Ennih and Liégeois, 2008).

Black and Liégeois (1993) stated that the 1.7 Ga to 1 Ga Mesoproterozoic quiescence allowed lithospheric thickening and craton formation of the West African Craton. The W.A.C., during the Neoproterozoic era had undergone various events leading to the construction of the present day geological framework. After the paleoposition of the W.A.C. during the Mesoproterozoic, the Neoproterozoic became an important period of evolution for the West African Craton.

The W.A.C. boundaries experienced Pan-African, Neoproterozoic to Early Cambrian transpression and transtension, intrusion of granitoids and extrusion of huge volcanic sequences in rocks such as those of the Anti-Atlas (Ouarzazate Supergroup). As a result of this tectonism, large sediment influxes were generated around the W.A.C. within the Peri-Gondwanan terranes with sedimentary sequences marked by distinctive zircon ages of 1.8–2.2 Ga and 0.55–0.75 Ga.

The West African Craton underlies the modern countries of Morocco, Algeria, Mauritania, Senegal, The Gambia, Guinea Bissau, Guinea, Mali, Burkina Faso, Sierra Leone, Liberia, Ivory Coast, Ghana, Togo and Benin.

2.2 THE EBURNEAN OROGENY

According to Dirks et al. (2003), sedimentation, volcanism and tectonism which occurred between 2.3 and 1.8 Ga, were the dominant events characteristic of the Paleoproterozoic geology of the African plate. These events describe the "Eburnean Orogeny" and have been recognized in Southern, Central and West African Cratons. These tectonic, metamorphic and plutonic events occurred during the Paleoproterozoic era between 2200-2000 million years ago, resulting in the Birimian domain of western Africa (Egal et al., 2002).

According to Vic and Billa (2015), the deposition and emplacement of these Birimian rocks date from 2230 Ma to 2060 Ma (for the younger magmatic rocks) and was driven by a protracted geodynamic evolution characterised by convergence and subduction processes. Rosa-Costa et al. (2003) also described the evolution to have occurred as a result of the convergence between a southern Guyana Shield Craton in Brazil and the Kenema-Man Craton of western Africa. Detailed studies of magmatism particularly in French Guyana (Delor et al., 2001) and Burkina Faso (Castaing et al., 2003), indicate oceanic subduction processes (Ganne et al., 2012) associated with oceanic magmatic arcs. This convergence caused the tectono-metamorphic and magmatic events in western Africa (Delor et al., 2001), termed the Eburnean orogeny which started circa 2220 Ma. The Eburnean orogenic event has been identified by two main deformational stages.

The Eburnean D1 tectono-metamorphic stage, is roughly estimated to date around 2120 Ma using ages from French Guyana, Ghana and Guinea, according to researchers like Delor et al. (2001) and Feybesse et al. (2006). This stage is associated with reverse faulting, foliation and metamorphism locally reaching upper greenschist to amphibolite facies. In southwest Ivory Coast (Ity-Toulepleu), where the San-Pedro Archean terrane is associated with the Man-Kenema Craton, D1 tectono-metamorphic events are notably intense (Triboulet and Feybesse, 1998).

The Eburnean D2 deformation stage, which occurred at about 2100 Ma according to Triboulet and Feybesse (1998), was due to an oblique convergence evolution, associated with transcurrent faulting along regional-scale shear zones. During the D2 stage, faults and associated folds were generally sub-vertical, with main sinistral kinematics and epizonal metamorphism and was retromorphic when the D1 stage was higher. At a very shallow level, major strike slip faults may have generated, pull-apart basins infilled by clastic rocks including sandstones and conglomerates; an example being the Toulepleu conglomerate, and volcanic epiclastic rocks. Later stages of deformation such as the D3 stage are limited and heterogeneous in western Africa. Late to post-orogenic magmatism is represented by muscovite-bearing granites (~2080 Ma), differentiated granites and syenites (Triboulet and Feybesse, 1998).

2.3. THE BIRIMIAN

The Birimian Paleoproterozoic terrane, also known as the Baoulé-Mossi Domain, outcrops south of the Man Shield of the West African Craton. The volcano-sedimentary belts in this terrane with associated Eburnean granitoids (Fig. 2.2) were formed between 2250 and 1980 Ma (Feybesse et al., 2006). It extends from the western half of Ghana into countries such as Côte D'Ivoire, southern Mali, Senegal, Burkina- Faso and west of Niger. Bonhomme (1962) established that the dominant structural grain of this terrane was formed during the Eburnean orogeny.

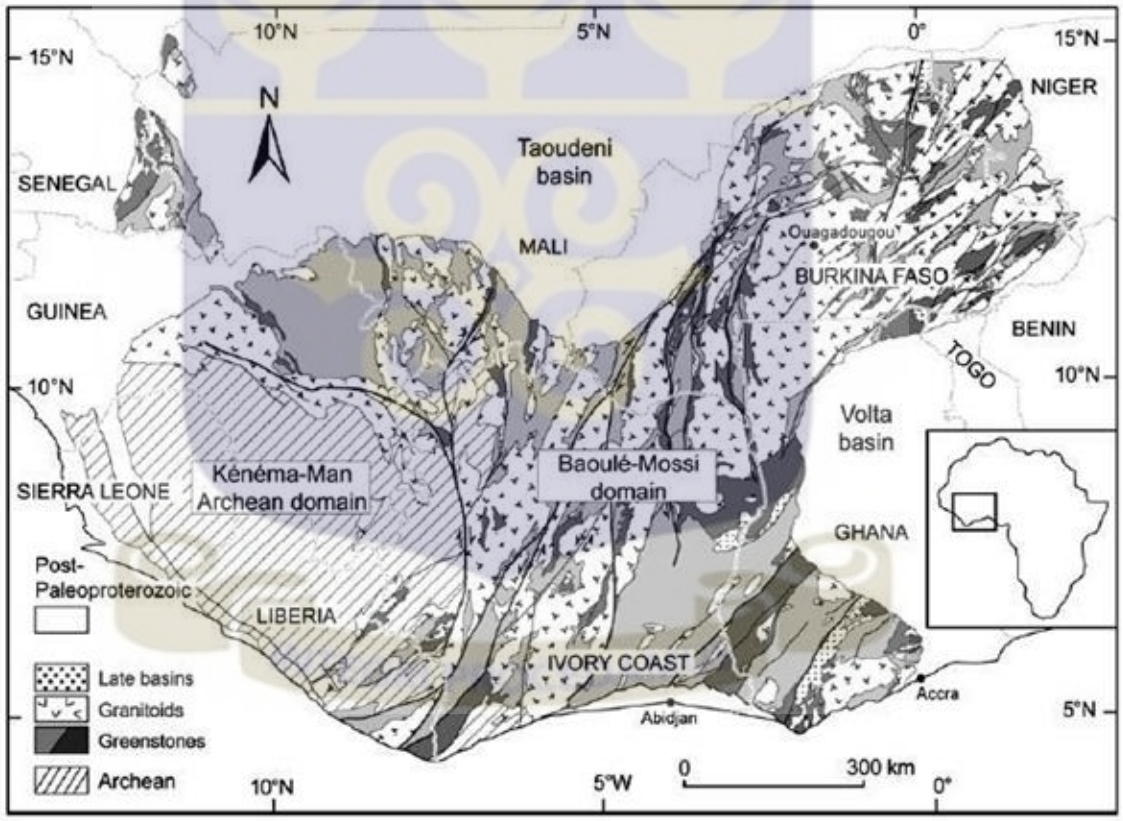

Figure 2.2 Geological map of the West African Craton (adopted from the BRGM SIGAfrique map, Milési et al., 2004); the Paleoproterozoic greenstones are divided into: light grey- intermediate to acid volcano-clastic and volcano-sediments, dark grey- mafic to intermediate lavas and volcanic.

The volcano-sedimentary belts in this terrane comprise of metasedimentary rocks; such as phyllites and graywackes, and metavolcanic rocks; such as the basalts-andesites series, which have been intruded by Eburnean granitoids and sometimes considered as separate units. The metavolcanic rocks are characterized by tholeiitic and/or calc-alkaline compositions. These volcanic formations are considered younger than the sedimentary sequences (Junner, 1935, 1940; Ledru et al., 1991; Milési et al., 1989, 1991).

Though, Leube et al. (1990), suggested that the volcanic sequences and sedimentary basins are contemporaneous lateral facies equivalents, while other researchers place the basalts and andesites at the base, overlain by flysch-type sedimentary sequences (Tagini, 1971, 1972; Bessoles, 1977; Vidal and Alric, 1994; Pouclet et al., 1996).

After numerous studies on the Precambrian greenstone belts, Baratoux et al. (2011) concluded on an immature volcanic arc setting represented by bimodal tholeiitic to calc-alkaline volcanism, with slight compositional differences existing with respect to the present-day island arcs. The tholeiitic basalts are considered older than the calc-alkaline series in the majority of these works.

The greenstone belts are significantly elongated probably as a result of intra-continental rifting according to research conducted by Leube et al. (1990), Rathamaro et al. (1988), Alric (1990) and Pouclet et al. (1996). These, as well as other contradictory interpretations of the evolution of these Birimian Paleoproterozoic rocks, have attracted a lot of scientific attention for nearly a century.

Birimian sedimentary basins occur abundantly across the whole Baoulé-Mossi domain. Vidal and Alric (1994) suggested that the basins unconformably overlay the older basement composed of predominantly tholeiitic volcanics and first generation of granitoids, while Hirdes et al. (1996) and Lüdtke et al. (1998) proposed that these basins are lateral equivalents and contemporary products of the volcanic islands.

Pouclet et al. (1996) and Pouclet et al. (2006) stated that the intracontinental basins formed at a later period in the tectonic history, on the consolidated tonalite-trondjhemite-granodiorite (TTG)-greenstone basement and were contemporaneous with calc-alkaline magma production. Voluminous plutonic activity contributed significantly to the growth of continental crust during the Eburnean orogeny.

2.3.1 Evolutional history of the Birimian Supergroup

The evolution of the Birimian began at the margin of the Archean Sao Luis Craton (SLC) around 2.35-2.30 Ga with plutonic activity and the deposition of volcano-sediments in basins resulting from the breakup of the Craton. Magmatic accretion reached its peak phase around 2.25-2.17 Ga with emplacement of huge quantities of juvenile basic-volcanic-plutonic rock accompanied by greywackes deposited no later than 2.22 Ga-that initiated the creation of crustal segments; such as the Kibi-Winneba, Sefwi and Ashanti belts (Villeneuve and Cornée, 1994). This was followed at around 2.16-2.15 Ga, by extensive monzonitic plutonism whose emplacement led to the formation of the first segments of the continental crust.

The transition period between the magmatic accretion and the Eburnean orogeny is marked by the development of the Sunyani, Kumasi-Afema and Comoe basins between 2.15 and 2.10 Ga. These are considered to be foreland basins in that, their flysch-like sedimentary fill was partly contemporaneous with the onset of the Eburnean orogeny at 2.13 Ga. According to Feybesse et al. (2006), the other basins, such as the Cape Coast basin, gradually formed over a period of time during various deformational processes. No substantial evidence concerning the Suhum Basin has been documented.

2.3.2. The Birimian in Ghana

The regional geology of southern and western Ghana (Figure 2.3) is comprised of thick sequences of steeply dipping metasedimentary rocks, alternating with metavolcanic units of Proterozoic age. These sequences, which belong to the Birimian Supergroup, extend approximately 200 km along strike, in a number of northeasterly trending belts.

The six main gold belts in Ghana are Kibi-Winneba, Ashanti, Sefwi-Bibiani, Lawra, Bui and Bole-Nangodi belts. These are separated by broad basins containing isoclinally folded dacitic volcaniclastics, wackes and argillitic sediments as well as granitoids. The broad intervening metasedimentary basins include; the Maluwe, Sunyani, Kumasi, Cape Coast and Suhum basins. Within the sedimentary basins, various lithofacies are distinguished.

Two contrasting concepts exist regarding the age relationship between the metavolcanics and the metasediments in Ghana. Junner in 1940, asserted that the sedimentary series occupied the upper position.

However, Tagini (1971) in Leube et al. (1990), and the francophone geologists believed that the metavolcanics are rather older than the metasediments. Leube et al. (1990) proposed a new version of the stratigraphy, where the lavas occur contemporaneously as lateral facies equivalent.

Concerning the tectonic model for the evolution of the lower Proterozoic rocks in Ghana, Leube et al. (1990) proposed a multi-rift or graben model with two distinct phases of deformation event, Eisenlohr and Hirdes (1992) suggested a single, progressive deformational event involving a series of deep seated, partly blind thrusts, possibly in a foreland basin setting.

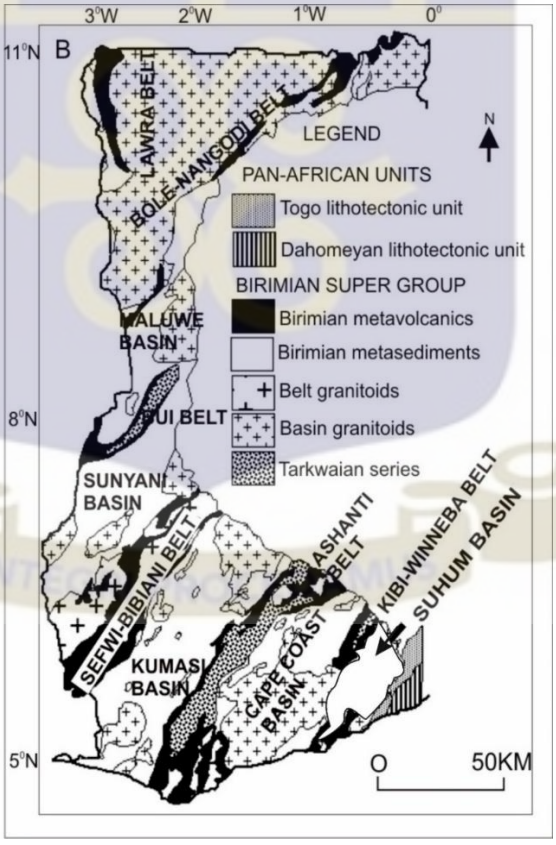

Figure 2.3 A modified geological map of the Birimian Paleoproterozoic rocks in Ghana showing the Suhum Basin (after Eisenlohr and Hirdes, 1992).

The tectonic evolution model of the Lower Proterozoic rocks in Ghana have generally invoked two deformation events. During the first event, the Lower and Upper Birimian rocks had undergone deformation, granitoid intrusions, upliftment and erosion with the accumulation of the resulting detritus, the Tarkwaian, in a series of grabens located within the volcanic belts. A second deformation event involving renewed folding (Ledru et al. 1988) or gravity tectonic processes (Leube et al. 1990) affected both Birimian and Tarkwaian rocks.

Feybesse et al., (2006), in his research proposed three phases of deformation regarding the Birimian terrane in Ghana, namely D_1, D_2 and D_3 deformations. The D_1 deformation was defined by S_1 foliations parallel to the axial plane of microfolds and by an L_1 stretching lineation. Penetrative fabrics developed during this stage vary according to the intensity of metamorphism and the relative proportion of co-axial strain associated with the deformation.

The D_2 deformational phase, represents the maximum strain, manifested by F_2 folds with horizontal or slightly plunging hinges, associated with a general east-northeast to west-southwest striking S_2 cleavages and north-east to south-west sinistral ductile faulting that variably included components reverse thrusting. D_3, is defined by folds generally associated with brittle shears, indicating that the crust was already exhumed to much higher structural levels.

2.4.1 The Kibi-Winneba Belt

The Kibi-Winneba volcanic belt (Figure 2.3) in southeastern Ghana is characterised by volcanic lobes, made up of basaltic flows, andesitic lavas, amphibolites, pyroclastics with granite–diorite plutonic suites and sedimentary rocks, with granitoids occupying intervening positions. Mafic plutonic bodies also intrude parts of the belt. This belt displays very similar lithological and structural characteristics to the volcanic belts located in western Ghana.

According to Anum et al. (2015), both the Birimian metavolcanics and metasediments are intruded by different types of granitoids. The most obvious feature in all the outcrops within this terrane is the presence of mafic enclaves, made up mostly of amphibolites and gabbros. The Kibi-Winneba belt is separated from the Ashanti belt to the west by the Cape Coast basin, and separated from the Pan-African mobile belt to the east, by the Suhum basin. Comparatively, the Cape Coast Basin has received more attention from researchers than the Suhum Basin, and thus has more documentation concerning the geology of these Birimian rocks.

Most areas in the Cape Coast Basin are mainly composed of metasedimentary rocks comprising tuffaceous metagraywackes with subordinate quartzites and interbedded gray and black phyllites and schists (Asiedu et al., 2004). Mafic to ultramafic lavas and sub-volcanic rocks are also common. In some portions of the Cape Coast Basin especially within the southeastern portions, the metasedimentary rocks are intruded by basin-type granitoids. Other post-Birimian intrusive rocks include granite, aplite, porphyry and pegmatite.

The Birimian rocks in the basin generally exhibit up to greenschist facies regional metamorphism. Both the metasedimentary rocks and the ultramafic intrusives close to granite batholith display various degrees of contact metamorphism. The rocks have been affected by low-grade metasomatic alterations, involving silicification and widespread formation of secondary chlorite and sericite.

So far recent studies conducted by a group of researchers through the Ghana National Geological Map Project (G.N.G.M.P.) in 2009, have concluded that the Suhum Basin is covered by;

1. Amphibolites originating partially as a result of contact metamorphism. These are Birimian protoliths which have been affected by Eburnean Tectono-metamorphic overprinting.
2. Locally migmatitic biotite gneisses and minor biotite schists; which may include garnets and/ or amphiboles. At the periphery of the granitoid plutons, gneissose rocks may also form. Results of radiometric studies conducted suggest ages of 2187±1Ma and 2165±9 Ma (Loh et al., 1999 and Hirdes and Davis, 1998).
3. Granitoid and biotite gneisses (2132±4 Ma), described as "Tamnean" protoliths also affected by affected by Eburnean Tectono-metamorphic overprinting.
4. Two-mica or muscovite granite and minor granodiorites (2088±1 Ma), which are locally leucogranitic.
5. Pre-Mesozoic mafic dolerite dyke, inferred from aeromagnetic data, dolerites, gabbros, basalts and subvolcanc rocks interbedded with minor volcaniclastics.

CHAPTER THREE

METHODOLOGY

This chapter describes the various stages employed in this research. It is divided into three (3) broad sub headings according to the different phases of the work done: Reconnaissance and Desk study, Field work and Laboratory work.

3.1. RECONNAISSANCE SURVEY AND DESK STUDY

The desk study and literature review were conducted before the reconnaissance survey and actual field work to ascertain previous work done throughout the Birimian terrane, especially the Birimian of Ghana, with emphasis on the metasedimentary rocks. At this stage, geological maps, books, journal articles, and all available publications were thoroughly studied to have a fair idea of the regional and local views of the Birimian, as well as various interpretations and models presented over the years.

The purpose of the reconnaissance survey was to have an idea of the available outcrops and their distribution throughout the study area, and to learn as much as possible about the geology of the study area. During this stage, all logistics such as base maps, eTRex Vista HCx Personal Navigator (GPS), field notebooks, geological hammers, measuring instruments, sampling bags and software needed for the research were acquired to aid in a successful execution of the project.

3.2. FIELD WORK

Field work mainly involved sampling of rocks for geochemical and petrographic analysis. Representative and oriented rock samples were obtained using geological hammers. This was done on three (3) field sheets at a scale of 1:50,000. More detailed rock sampling followed after the reconnaissance survey.

Since the rocks of interest were the basin rocks, coordinates of their possible locations were extracted from the recent geological map of Ghana (GSD, 2009) and keyed into the Global Positioning System (GPS) and used on the field.

In all, about 45 fresh representative samples were obtained from the field to characterize the rocks of the Suhum basin. Figure 3.1 shows the various sampling points represented by black circles, with the various areas where the schists were observed indicated by the short dashed circles. On the field, care was taken to observe the pegmatites occurring in very close contact with the schists. Digital photographs were taken and hand specimen descriptions were made and documented.

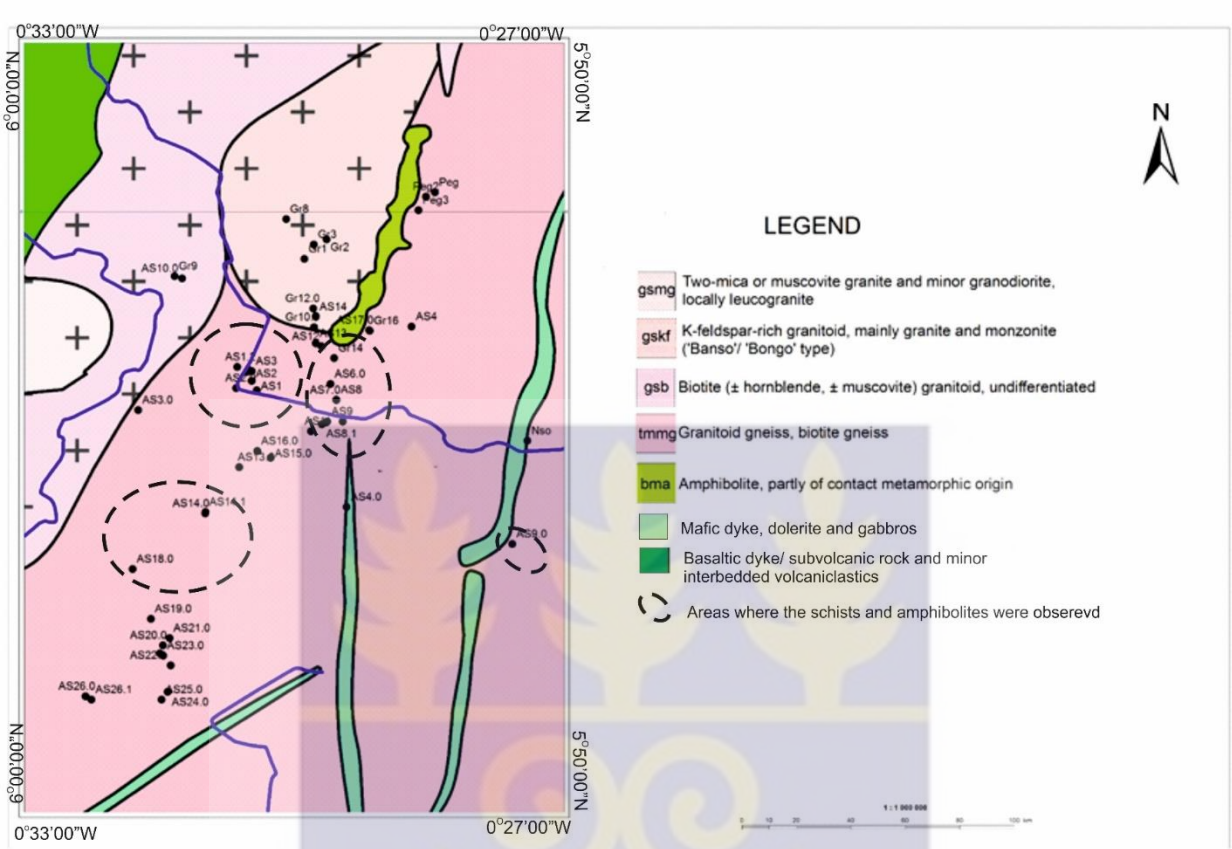

Figure 3.1 A geological map of the study area located at the northeastern portion of the Suhum basin, South-eastern Ghana; showing the sampling stations. Circles showing areas where the schists were observed. (extracted from the Ghana National Geological Map Project; 2009).

3.3. POST FIELD WORK

3.3.1. Thin Section Preparation

Thin sections were prepared at the Petrographical Laboratory in the Department of Earth Science, University of Ghana. Selected samples were cut with a diamond blade rock saw to small, thin rectangular billets with dimensions which could fit on a glass slide (46 by 26 millimetres). One side of the billet was labeled using a permanent marker whilst the unlabeled side was polished on a lap wheel to rid the surface of abrasions from the saw, pits, scratches and intergranular relief. Slurry of 400 grit carborundum was placed on the wheel lap to aid the grinding and polishing process. After the surface was smooth enough, the billet was washed and dried on a hot plate. Using a spatula, a small portion of epoxy was placed on the slide whilst on the hot plate. The glass slide and billet were put together and warmed to allow the billet to cure, after which it was allowed to cool and then trimmed.

On a glass plate, a slurry of water and polishing powder was made and the section with the rock side down was ground to reduce the thick parts. The section was rinsed with water frequently to check the thickness intervals as the grinding proceeded. A finer slurry of water and polishing powder was made and the procedure was repeated until the desired thickness, normally 30 microns was achieved. To test whether the thickness was sufficient, the slide was viewed under the light polarizing microscope for common minerals such as quartz and feldspars. As the sample got thinner, the interference colours and for that matter the birefringence of feldspar, for example, would change from bright colours to gray which was indicative that the section was thin enough. Finally, a cover slip was cemented onto the rock and the glass slide properly labeled.

3.3.2. Thin Section analysis

Thirty (30) samples were prepared into thin sections for petrographical and microstructural studies. During this activity, the physical and optical properties of minerals were studied using the Leica DM750P polarising microscope. Some of these properties included grain form or shape, colour, relief, pleochroism and interference colours. To identify the various rock types, the textures and mineral associations were studied.

The minerals were examined under plane and crossed polarised light to highlight the mineralogical and textural features of the samples. Various magnifications (x25) were used in investigating the samples in the thin sections. A low magnification of x35 was used in identifying textural and structural orientations whilst the intermediate magnification was used in viewing the mineral grains and other minute characteristics such as mineral cleavages and haloes. Photomicrographs were also taken to record special features for further interpretations.

3.3.3. Geochemical Analysis and Interpretation

In all, twenty-five (25) fresh, homogenous and representative samples were selected for whole rock geochemical analysis. Selected samples were cut into cubes and sent to ALS laboratory in Vancouver, Canada for whole rock geochemical analysis. Standard procedures were followed during the sample preparation which commenced at the Australian Laboratory Services (ALS) laboratory outlet in Kumasi, Ghana, before being transported to ALS in Vancouver, Canada. The rock chips were weighed and crushed to fine powder below 2mm (<70%).

A riffle splinter was used to split samples which were later pulverized through < 75µm (pulverize split to 85%). Crushing QC test and Pulverizing QC test were carried out using standard procedure at the ALS laboratory.

Whole rock major element analysis was then carried out using ICP-AES at the ALS laboratory in Vancouver following standard procedure accredited to ISO/IEC 17025-2005 standards. Results were delivered via email, and the necessary geochemical diagrams were plotted to aid in data interpretation.

Several computer softwares including Microsoft Excel 2016, MapInfo, Deltagraph 5.6.5, Geological Data Toolkits (GCDkit) 4.1 and CorelDraw X7 were used for data analyses and for plotting the maps and geochemical diagrams.

CHAPTER FOUR

RESULTS

4.1. PETROGRAPHY

This section outlines the hand specimen as well as microscopic descriptions of the samples obtained from the field. Characteristics such as the rock texture, mineralogy, alteration and structures, will be the main highlights used in this petrographical analysis. Data from the field concerning the petrography, rock relations and petrogenesis of the schists and amphibolites sampled are presented.

A total of forty-five (45) rock samples were collected from areas such as Alema, Amfaso, Akwatikurom, Dorkrokyewa, Duodukurom, Coaltar, Kwamekyerekurom, Oparekurom, Obundanfo and Yaa Apem within the study area. The main lithologies sampled include schists and amphibolites.

From the petrographical analysis, four (4) types of rocks were identified. These are hornblende-biotite schist, biotite schist, muscovite-biotite schist and amphibolites. The schists and amphibolites occur in close relations as shown in Figure 3.1 and thus, are grouped and listed as follows;

1. The Schists: Biotite Schists (2 samples), Hornblende-biotite schists (6 samples) and muscovite-biotite schists (2 samples).
2. Amphibolites (6 samples).

4.1.1. Schists

Generally, these rocks were encountered mostly in close relations with the pegmatites which occurred in the study area. Some common structures found within these rocks include foliations, veins and few joints. Very fresh samples were difficult to obtain as most of the rocks, especially those occurring along the road cuts were strongly weathered.

The pegmatites were observed as marker horizons aiding in easy identification of the schists. Most of the schists are generally fine grained, foliated and composed of mafic minerals as compared to the pegmatites which are coarse grained, non-foliated and composed of felsic minerals; such as quartz and K-feldspar. The pegmatites were seen occurring as "dykes" and hence, are generally believed to be younger than these schists.

The schists were encountered;

1. Occurring on their own; as was observed in the case of the biotite schists within the Kua river in Oparekurom, indicated in Figure 3.1 as station AS1.
2. Occurring together with the pegmatites; as in the case of the rocks observed along the roadcut around towns such as Yaa Apem and en route from Tetekasom through to Dorkrokyewa.

Three types of schists were identified and selected per their distinctive characteristics owing to the different mineral compositions. A summary of the visually estimated mineral compositions of these schists is listed in Table 4.1a.

Table 4.1a Visually estimated mineralogical compositions of the various schists identified within the study area.

Rock name		**Biotite Schists**		**Hornblende-Biotite Schists**					**Muscovite-Biotite Schists**	
Sample No.		**AS01A**	**AS09B**	**AS05B**	**AS06A**	**AS06E**	**AS08.1A**	**AS08.1C**	**AS014A**	**AS014C**
%										
Amphiboles		20	-	25	25	25	30	20	-	-
Feldspars		-	10	10	15	<5	13	22	15	<10
Micas	Biotites	25	45	40	35	35	40	35	40	35
	Muscovites	-	5	-	-	-	-	-	10	10
Quartz		10	35	20	25	19	17	23	35	45
Chlorites		30	-	-	-	15	-	-	-	-
Sericites		15	-	<5	-	-	-	-	-	-
Opaque Minerals		-	-	-	-	<1	-	-	-	-

4.1.1.1 Hornblende-biotite schist

These dark coloured rocks were found mostly in Oparekurom, Duodokrom, Alema, Dorkrokyewa and Kwame Kyerekurom. Generally, the colour of these fine grained rocks ranged from dark grey to dark green. The primary minerals forming these rocks include biotites (35-40) %, amphiboles (20-30) %, quartz (17-25) % and plagioclase feldspars (5-22) %. These mineral compositions varied within the six samples observed, though the biotites tend to occur abundantly within the rocks. A few opaque minerals (<1%) can also be observed within these rocks.

The quartz grains are subangular. The foliated texture of these rocks can be attributed to the elongation of the amphiboles within some of these rocks (Figure 4.2. D and F) aligned with the platy nature of the biotites in the rocks (Figure 4.2. A, B and E). In thin section (Figure 4.2.), the rocks show heterogeneous characteristics such as non-uniform grain sizes and orientations indicating that these rocks were probably formed as a result of inputs from different point sources.

The percentage of quartz is relatively low as compared to the unstable minerals (e.g. hornblendes and biotites), a sign of low textural maturity. The incipient growth of the micas within these rocks is most likely as a result of the metamorphism of a possible matrix, is also an indication of immaturity. Most of the minerals that make up the bulk mineralogical composition of the rocks are mostly least resistant to weathering processes. This is an implication that the rocks exist relatively close to their original sources. There is an occurrence of some levels of epidotization of the amphiboles, chloritization of the biotites, as well as sericitization of the feldspars within these rocks.

Also, the heterogeneous, as well as textural immaturity of the minerals that make up these rocks, show evidence of lack of transportation of the rock constituents from the original source areas. From the varying mineralogical compositions (Table 4.1a) of the hornblende-biotite schists from the study area, an input from mafic and intermediate source rocks can be observed.

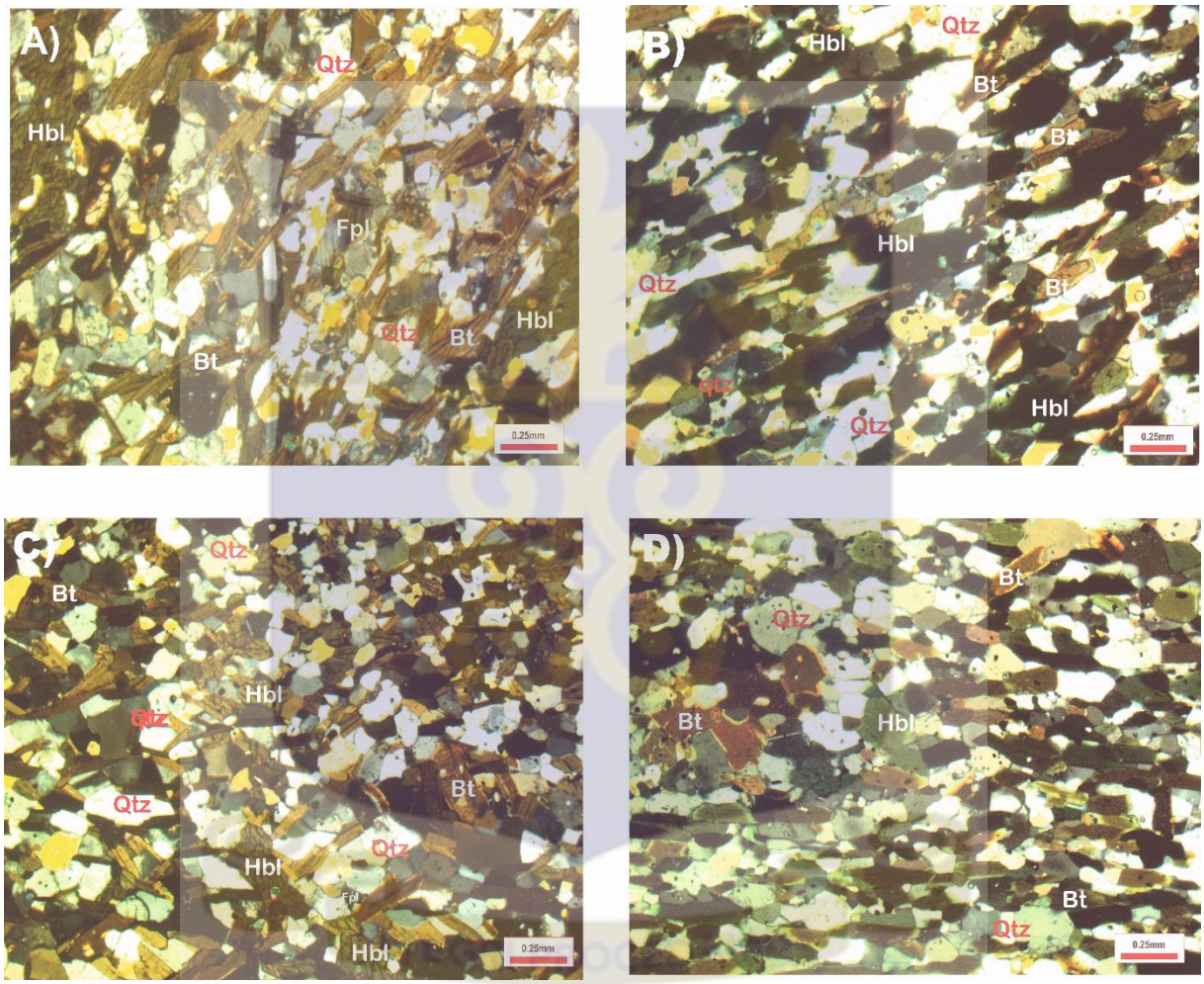

Figure 4.1. Photomicrographs of the different types of hornblende-biotite schists observed within the study area; A- Duodukurom, B- Oparekurom, C- Duodukurom and Dorkrokyiwa, D- Kwamekyerekurom. Photomicrographs taken under crossed polarised light; Bt-biotites, Qtz-quartz, Fpl-plagioclase feldspars and Hbl-hornblendes.

4.1.1.2 Biotite schist

These dark green coloured foliated rocks were found mostly in Akwatikurom, Oparekurom (especially within the River Kua) and Amfaso. The rocks are strongly foliated and fine to medium grained.

The primary minerals found within these rocks include biotites (25-45) %, quartz (10-45) %, hornblendes (20%), plagioclase feldspars (10%) and muscovites (5%). Subangular quartz grains were observed within these rocks. From the thin section, the quartz and feldspars occur as constituents of the original rock with the micas occurring as overgrowths in Figure 4.3; implying that the micas were not part of the formation of these rocks from the initial stages and may have formed as a result of the metamorphism of already existing matrix.

Also, heterogeneity, especially with respect to grain sizes and orientations, can also be observed. The platy nature of the micas in the rocks contribute primarily to the foliated nature observed within these rocks as the minerals tend to be aligned in a preferred orientation. Chloritization of the biotites was also very obvious within the rocks (Figure 4.3.B), as the partial alteration of some the brown biotites to green coloured chlorites can be observed leaving the original pseudomorphs of the biotites still visible.

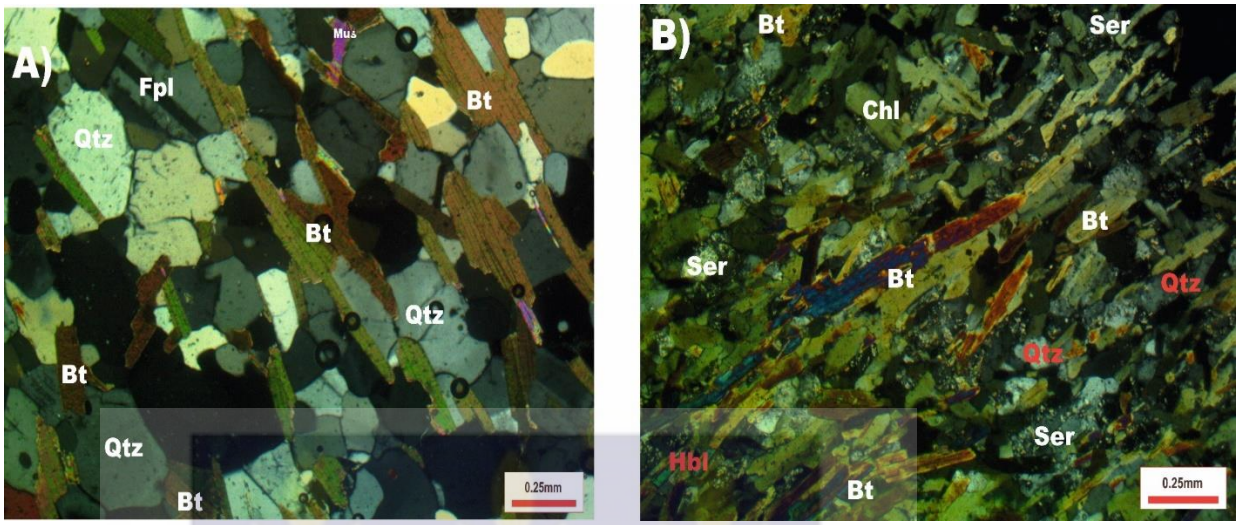

Figure 4.2. Photomicrographs of the different types of biotite schists observed within the study area; A-Amfaso and B- Oparekurom. Photomicrographs taken in crossed polarised light; Bt-biotites, Ser- sericites, Qtz- quartz, Chl-chlorites and Mus-muscovites.

4.1.1.3 Muscovite-biotite schist

These strongly foliated dark coloured rocks were observed to have outcropped mostly within Akwatikurom and Amfaso. These rocks were observed at some locations in contact with the pegmatites as indicated in Figure 4.4B (thick black line showing contact).

The primary mineral constituents within these rocks include quartz (35-45) %, alkali feldspars (in minute quantities) and plagioclase feldspars (10-15) % and micas (biotites and muscovites). Sericitization of the feldspars can also be observed within the rocks (Figure 4.3B). Subangular quartz grains also exist within these rocks, with the platy nature of the micas clearly resulting in the foliated nature of these rocks. A few grains are also elongated and aligned to the orientation of the micas.

The heterogeneous nature of the rock is also obvious as most of the mineral grains especially the quartz shows varying grain sizes and orientations. Contrary to the first two types of schists, the muscovite-biotite schists, show higher degrees of mineralogical maturity and source rock weathering. The maturity may also be accounted for by the higher percentages of quartz.

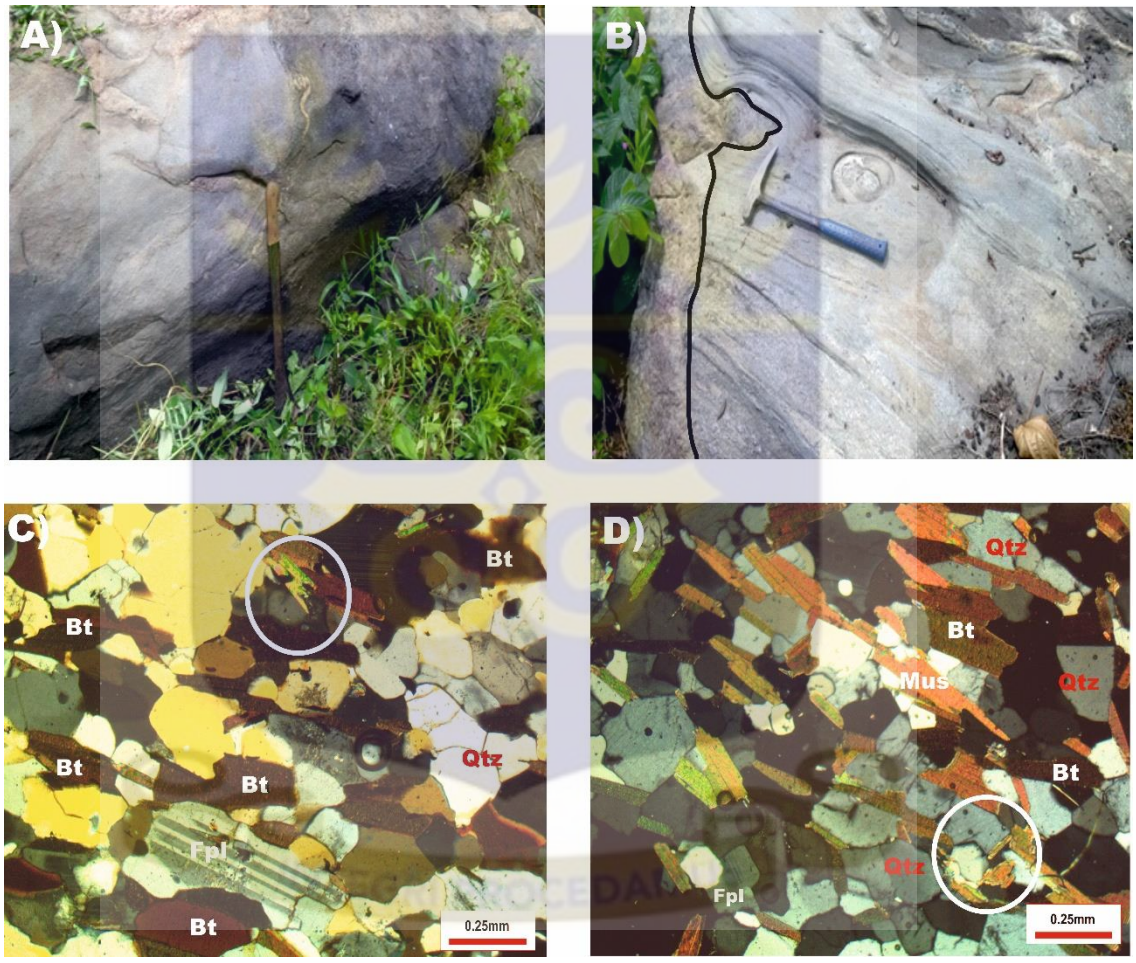

Figure 4.3. Field photographs A and B showing the muscovite-biotite schists outcropping within the study area; thick line in B) showing the contact between the schist and the pegmatites. Photomicrographs; C and D-Akwatikurom; with circular insets showing the muscovites within the thin sections. Photomicrographs taken under crossed polarised light. Bt-biotites, Mus-muscovites, Fpl-plagioclase feldspars, Qtz-quartz.

4.1.2. Amphibolite

Also observed among the lithologies within the study area are the amphibolites. These are one of the most abundant rocks identified within the study area, outcropping within Duodokrom, Alema and Dorkrokyewa. The primary minerals within these rocks are amphiboles (hornblendes), pyroxenes and plagioclase feldspars. Secondary minerals such as quartz, epidotes (Figure 4.5. B, D and E), chlorites (Figure 4.5. E) and sericites were also observed as a result of partial alteration or replacement of the primary minerals.

Silicification was also very obvious within some of these rocks as some quartz veins were clearly seen. The rocks are generally massive and were generally strongly altered. A few of the hornblendes exhibited some degrees of ferruginous weathering. A summary of the visual estimates of the mineralogical compositions of the different amphibolites sampled from the study area are given in Table 4.1b.

Table 4.1b. Visually estimated mineralogical compositions of the various amphibolites identified within the study area.

Rock Name	**AMPHIBOLITES**					
Sample No.	**AS05A**	**AS05C**	**AS015A(18)**	**AS018A**	**GR014A**	**GR014B**
%						
Amphiboles	75	85	75	65	85	75
Feldspars	-	-	-	12	-	-
Pyroxenes	-	-	-	-	4	-
Quartz	8	8	-	14	5	<5
Chlorites	-	-	5	-	-	<5
Epidotes	-	-	10	9	-	-
Sericites	12	7	9	-	6	15
Carbonates	4	-	-	-	-	-
Opaque Minerals	<1	<1	<1	<1	<1	<1

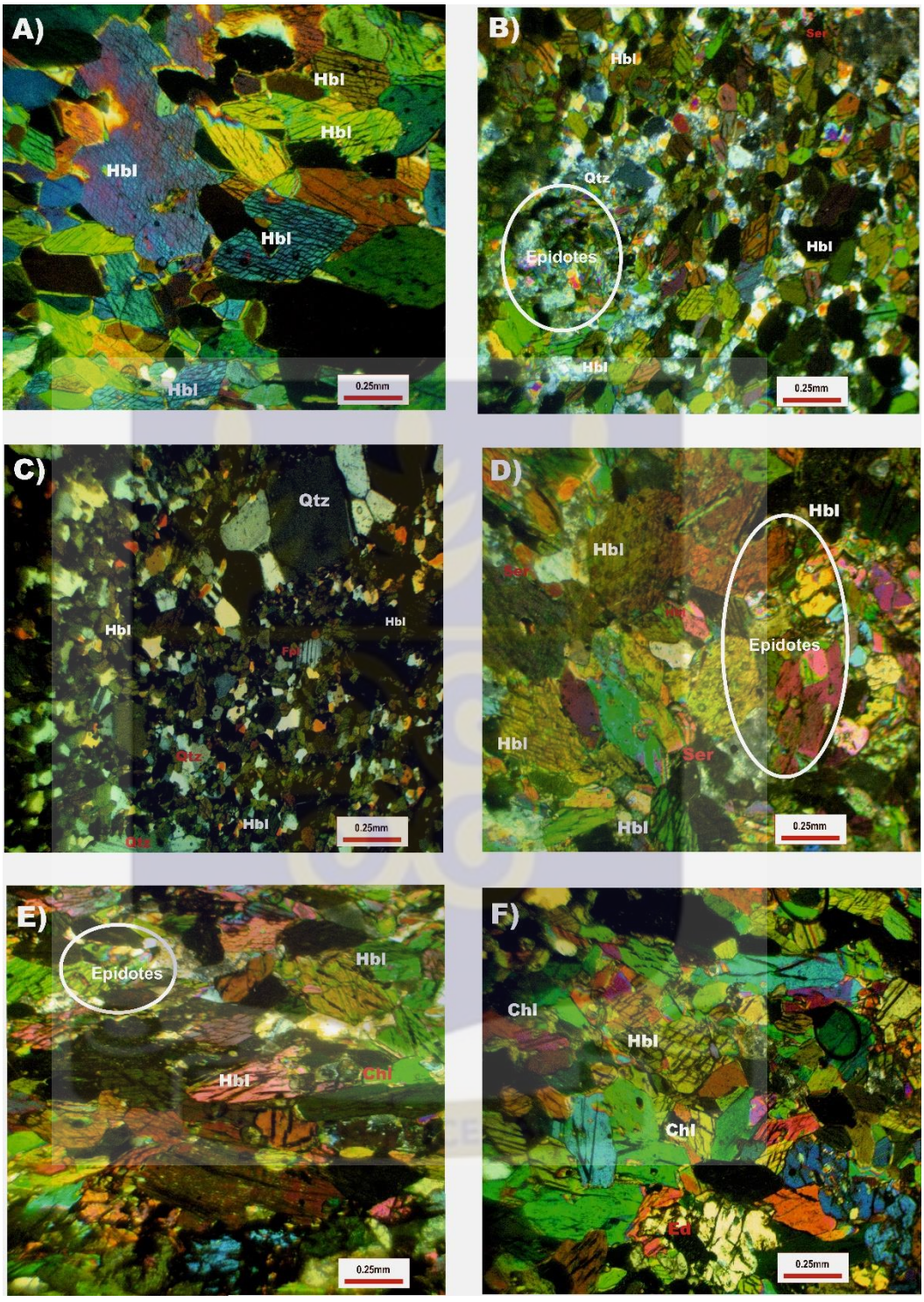

Figure 4.4. Photomicrographs of the different types of amphibolites observed within the study area; A- GR014A, B- GR014B, C- AS018A, D- AS015(18), E and F- Duodukurom and Dorkrokyiwa. Hbl-hornblende, Ed-edenite, Ser-sericites, Chl-chlorite and Qtz-quartz.

4.2. STRUCTURES

The structures that characterised the rocks within the study area include veins, joints, foliations and mineral lineations. The structures observed in the study area were mostly microscopic in scale. The veins (Figure 4.6.) within these rocks is an indication of remobilization of minerals as a result of metamorphism. The presence of foliations (Fig. 4.7.) is also an indication of metamorphism, possibly prograde metamorphism, and deformation occurring within these rocks. The joints and mineral lineations occurring within the rocks in the study area also indicate the occurrence of some degrees of deformation.

Generally, the structures observed within these rocks are an indication that the rocks have undergone some degrees of metamorphism as well as deformation. Characteristics such as the elongation of minerals such as the amphiboles (schists) and the micas within the schists, are an indication of regional metamorphism occurring.

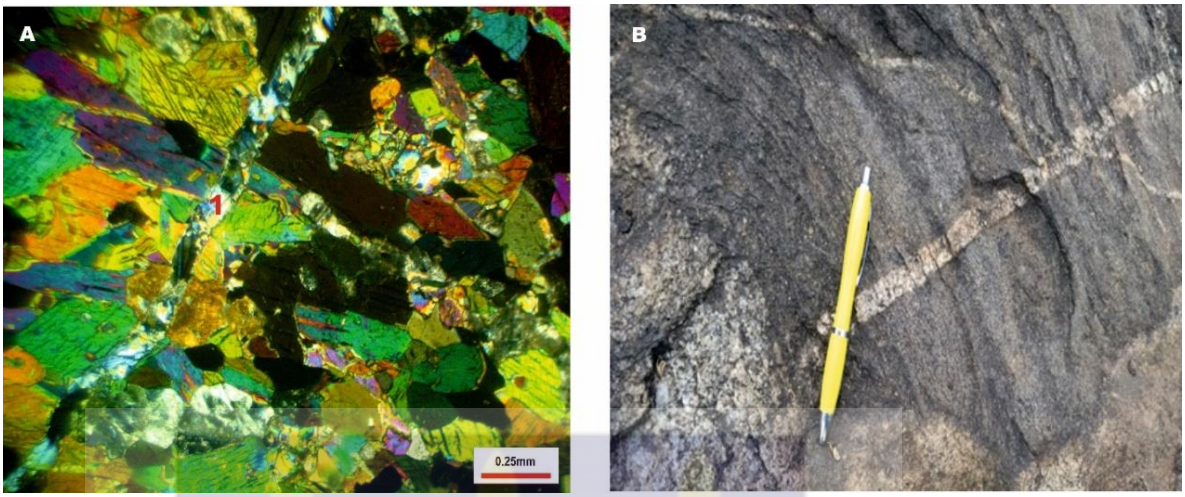

Figure 4.5. A. Photomicrograph of a rock within the study area showing clearly a vein. B. Photograph of a vein as well as veinlets observed within an outcrop.

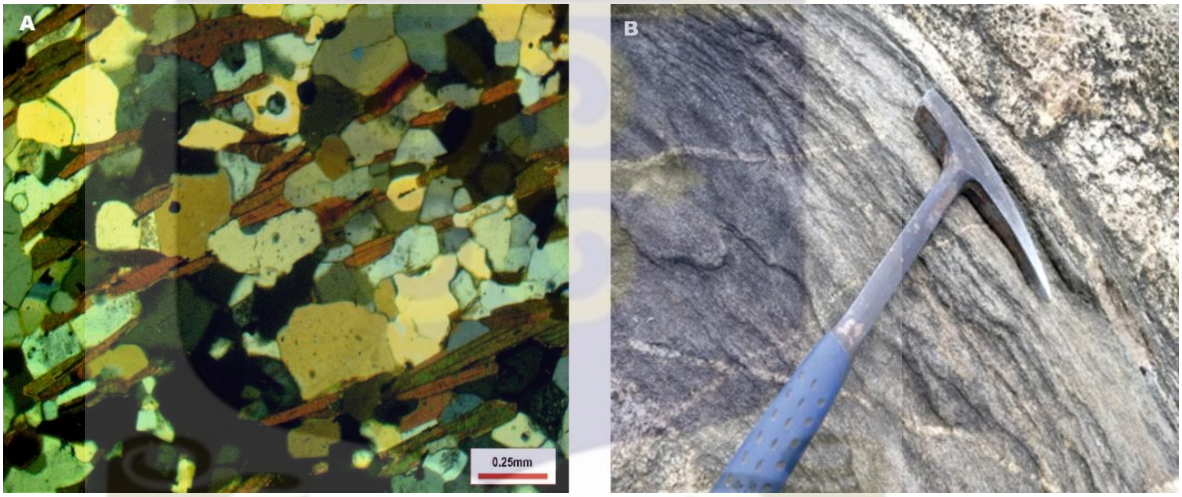

Figure 4.6. A. Photomicrograph showing foliations (schistosity) within a rock from the study area. B. Photograph of foliations observed within an outcrop.

4.3 MAJOR AND TRACE ELEMENT GEOCHEMISTRY

Table 4.2. (a and b) represents the major and trace element data for sixteen (16) rock samples from the study area. The samples are made up of ten (10) schists and six (6) amphibolites.

4.3.1 Major element geochemistry

4.3.1.1 Schists

The schists from the study area exhibit significant variations in their major element compositions; characterized by SiO_2 contents of 47-72 wt%, TiO_2 of 0-2 wt%, Al_2O_3 of 11-16 wt%, Fe_2O_3 of 4-15 wt%, MgO of 1-10 wt%, CaO of 2-13 wt%, Na_2O of 1-4 wt%, K_2O of 0-3 wt% and P_2O_5 of 0-1 wt% (Table 4.2 a).

From the major element data acquired, the schists can be classified into two groups based on their percentage weights of SiO_2. The schists containing <55 wt% of SiO_2 such as the biotite schists (AS01A and AS09B) and some of the hornblende-biotite schists (AS01B, AS05B, AS06A, AS06E) with relatively lower to immediate percentages of SiO_2, Al_2O_3, Na_2O, K_2O, P_2O_5 and relatively higher Fe_2O_3, MgO, CaO and TiO_2, these rocks can be classified as derived from intermediate to mafic rock sources.

Conversely, two hornblende-biotite schists (AS08.1A and AS08.1C) and muscovite-biotite schists (AS014A and ASO14C) contain >60 wt% SiO_2 and can be classified as rocks derived from felsic rock sources. All the schists from the study area show oxides such as Fe_2O_3, CaO, MgO, MnO and TiO_2 having strongly negative correlations with SiO_2, with a contrary positive correlation of Na_2O with SiO_2. The High Field Strength Elements for the schists also show very strong correlations with zirconium (Figures 4.8., 4.9. and Tables 4.3).

Table 4.2a. Major and trace element compositions of the schists identified within the study area.

Sample No.	AS01A	AS09B	AS01B	AS05B	AS06A	AS06E	AS08.1A	AS08.1C	AS014A	AS014C
Rocks	Biotite schists		Hornblende-biotite schists						Muscovite-biotite schists	
wt%										
SiO_2	48.3	50	50.2	47.3	55.1	54.8	62.2	61.8	67.7	71.3
Al_2O_3	13.75	13.1	14.1	11.1	13.75	13.75	12.9	13.25	15.9	13.7
Fe_2O_3	13.3	12.5	13	12.25	15	14.95	11.2	10.75	4.98	4.88
CaO	11.3	11.45	11.15	13	6.61	7.08	4.34	5.09	2.05	2.19
MgO	6.33	5.94	5.99	9.6	2.14	2.02	1.31	1.03	2.04	1.44
Na_2O	2.89	2.78	1.6	1.99	2.8	2.93	2.87	3	3.67	3.8
K_2O	0.66	0.51	0.99	0.49	1.38	1.02	2.26	1.92	2.8	1.87
Cr_2O_3	0.02	0.01	0.05	0.08	0.01	0.01	0.01	0.01	0.01	0.01
TiO_2	1.11	1.37	0.91	1.26	1.49	1.46	0.91	0.86	0.55	0.55
MnO	0.23	0.18	0.22	0.19	0.24	0.25	0.17	0.2	0.07	0.06
P_2O_5	0.13	0.11	0.11	0.46	0.61	0.59	0.3	0.25	0.24	0.13
SrO	0.02	0.03	0.02	0.07	0.02	0.03	0.02	0.03	0.04	0.04
BaO	0.02	0.01	0.02	0.03	0.04	0.04	0.07	0.07	0.09	0.06
LOI	1.33	0.55	0.89	1.16	0.35	0.26	0.33	0.26	1.23	0.62
Total	99.39	98.54	99.25	98.98	99.53	99.18	98.88	98.51	101.37	100.65
ppm										
Co	55	43	48	54	19	19	9	7	13	10
Ni	77	67	109	311	9	6	4	2	18	21
Pb	2	2	4	6	12	10	8	12	15	11
Sc	42	35	39	41	29	28	20	19	9	9
Zn	106	91	96	109	190	182	199	211	74	82
Ba	170	106	164.5	232	402	395	697	706	870	617
Ce	18.4	17.6	17.1	104.5	120	116	151	165.5	81.4	68.6
Cr	140	100	340	590	30	20	20	20	50	70
Cs	0.7	0.16	2	0.26	3.4	1.83	10.15	5.83	19.75	16.9
Dy	4.48	5.49	3.86	6.11	13.8	13.4	15.5	17.6	3.57	2.59
Er	2.81	3.2	2.37	2.49	7.86	7.97	9.56	10.7	1.84	1.3
Eu	1.21	1.55	0.84	3.45	3.7	3.54	3.51	3.82	1.15	1.06
Gd	4.09	5	3.68	9.72	14.55	13.85	15.4	16.9	5.02	3.29
Hf	1.9	2.6	1.8	3.5	9.6	9.3	13.9	15.5	4.6	4.9
Ho	0.96	1.12	0.8	1.08	2.67	2.76	3.27	3.73	0.7	0.47
La	7.8	10.1	7.4	41.1	58.3	52.9	70.3	76.6	40.8	28.7
Lu	0.38	0.4	0.32	0.3	1.07	1.16	1.35	1.6	0.23	0.16
Nb	3.4	4	3.3	5	31.8	32.3	37.1	42.5	11.9	8.2
Nd	12.3	16.1	10.7	64.5	66.6	60.5	74.1	80.8	34.5	25.8
Pr	2.54	3.27	2.29	14.5	15.9	14.45	18.4	19.8	9.12	6.69
Rb	23.3	7.3	25.6	8	52.1	30.6	92.7	62.5	112.5	119.5
Sm	3.42	4.36	2.89	12.85	13.8	13.4	15.8	17	6.22	4.45
Sr	237	296	228	632	225	250	212	251	346	422
Ta	0.1	0.2	0.1	0.2	2.1	2	2.3	2.6	0.6	0.6
Tb	0.71	0.87	0.62	1.17	2.22	2.18	2.45	2.76	0.67	0.47
Th	0.64	0.42	0.83	1.65	6.67	6.56	9.5	10.7	7.09	5.55
Tm	0.41	0.43	0.36	0.37	1.11	1.16	1.32	1.59	0.27	0.16
U	0.19	0.16	0.19	0.49	1.72	1.75	2.54	2.83	2.26	1.9
V	325	383	274	235	48	45	26	24	91	63
Y	24.4	29.1	21.3	27.4	71.6	74.2	88.2	99	18.8	11.8
Yb	2.58	2.68	2.31	2.16	7.09	7.41	9.1	10.65	1.86	1.04
Zr	69	93	70	134	379	386	575	649	174	182

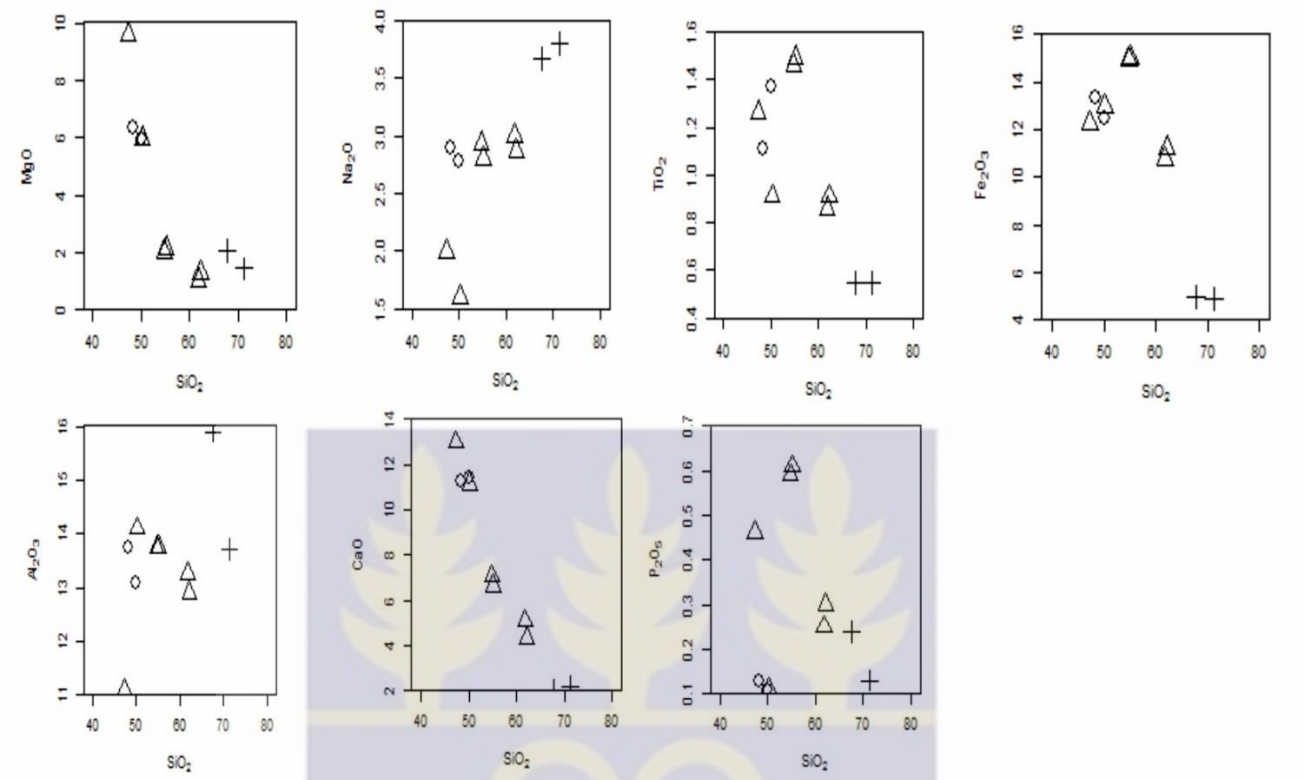

Figure 4.8. Selected major element–SiO_2 plots for the metasedimentary rock samples from the study area; the Biotite schists- Circles, Hornblende-biotite Schists-Triangles and the Muscovite-biotite schists- Cross.

The Loss of Ignition (LOI) values, the representative percentage weights, give a measure of the fluid contents, mobile elements and the degree alteration of the rocks was also taken into consideration. The Loss of Ignition values for the studied schists are generally low (0.26-1.33) an indication that these rocks have undergone relatively low degrees of alteration.

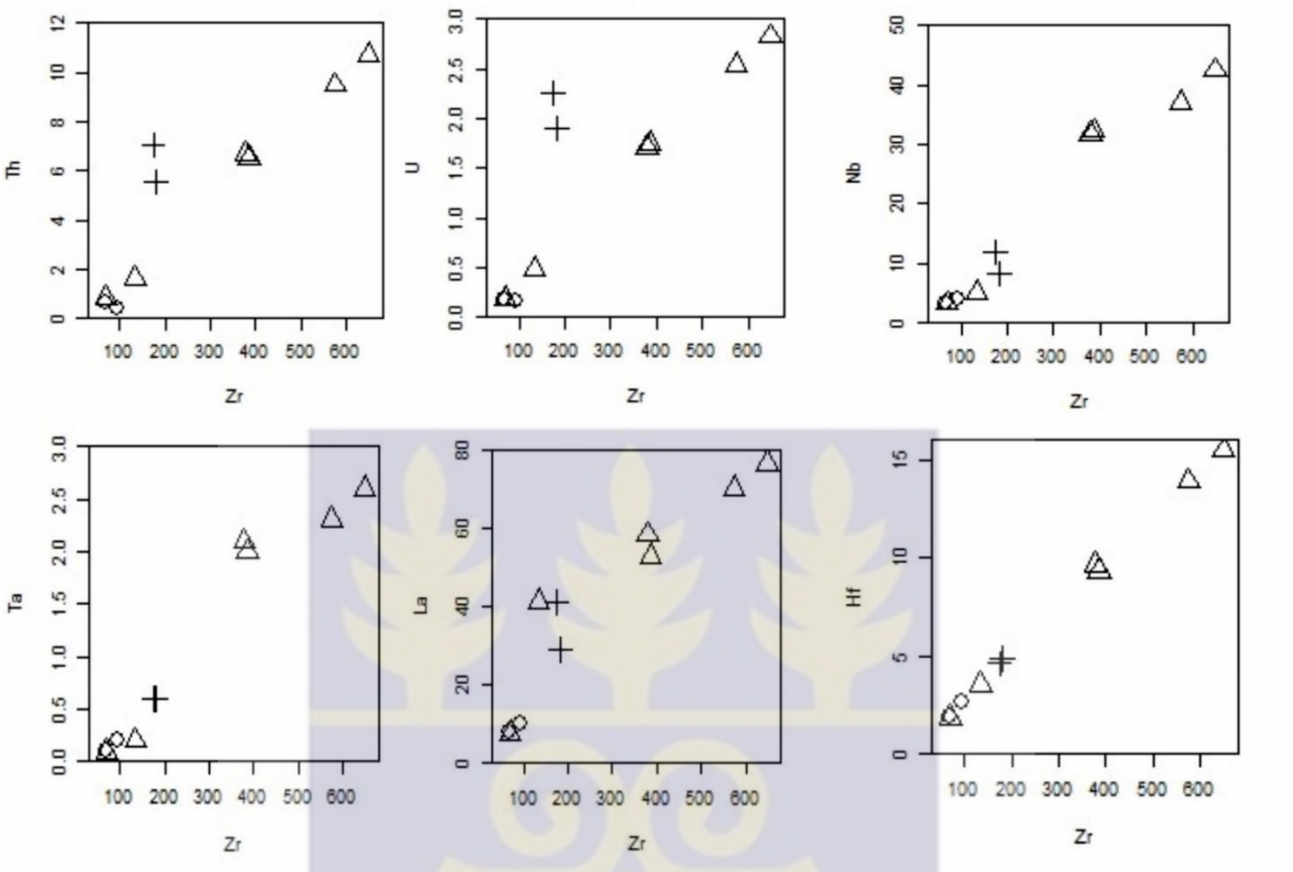

Figure 4.9. The High Field Strength elements (HFSEs)–SiO_2 plots for the schists from the study area; the Biotite schists- Circles, Hornblende-biotite Schists-Triangles and the Muscovite-biotite schists- Cross.

Table 4.3 Pearson correlation matrices for the major and High Field Strength Element compositions of the schists in Table 4.2 a.

(a)	SiO_2	Al_2O_3	Fe_2O_3	CaO	MgO	Na_2O	K_2O	TiO_2
SiO_2	1							
Al_2O_3	0.47709	1						
Fe_2O_3	-0.8155	-0.4051	1					
CaO	-0.9677	-0.5441	0.67459	1				
MgO	-0.8044	-0.5153	0.337	0.90136	1			
Na_2O	0.79917	0.49308	-0.6621	-0.8038	-0.6867	1		
K_2O	0.89163	0.5684	-0.6893	-0.9229	-0.7804	0.63403	1	
TiO_2	-0.7466	-0.4461	0.89093	0.61846	0.35021	-0.4517	-0.7178	1

(b)	Hf	La	Nb	Ta	Th	U	Zr
Hf	1						
La	0.935994	1					
Nb	0.975871	0.919455	1				
Ta	0.971637	0.912787	0.997091	1			
Th	0.911154	0.911421	0.88603	0.882939	1		
U	0.840056	0.859243	0.804179	0.803765	0.98687	1	
Zr	0.999388	0.931058	0.975465	0.969362	0.903981	0.830236	1

4.3.1.2 Amphibolite

The amphibolites from the study area exhibit significant variations in their major element compositions; characterized by SiO_2 contents of 47.2-48.9 wt%, TiO_2 of 0.9-2.29 wt%, Al_2O_3 of 10.8 -15.8 wt%, Fe_2O_3 of 10.4 -15.8 wt%, MgO of 3.93 -9.9 wt%, CaO of 9.89 -14.9 wt%, Na_2O of 1.32-2.76 wt%, K_2O of 0.43-0.53 wt% and P_2O_5 of 0.09-0.45 wt% as is shown in Table 4.2.b.

The SiO_2 values ranging from (47.2-48.9) % with a mean value of 48.15%, which fall within the 48-50% silica undersaturated interval of Ewart (1982). They are also characterized by low Al_2O_3 (10.8-15.8%), MgO (3.93-9.9%), K_2O (0.43-0.56%) and MnO (0.19-0.25%); and relatively high TiO_2 (0.9-2.29%), CaO (9.89-14.9%) and Fe_2O_3 (10.4-16.1%). The amphibolites are generally undersaturated in silica (mean value of 48.15%).

Table 4.2b. Major and trace element compositions of the amphibolites identified within the study area.

Sample	AS05A	AS05C	AS015A(18)	AS015B(18)	GR014A	GR014B
wt%						
SiO_2	47.2	48.7	48.8	48	48.9	47.3
Al_2O_3	11.25	10.8	14.65	14.4	14.15	15.8
Fe_2O_3	12.25	12.1	15.9	16.1	10.4	11.85
CaO	12.95	13.05	9.89	9.96	14.9	13.35
MgO	9.6	9.9	3.93	4.02	5.84	5.85
Na_2O	1.94	1.99	2.76	2.69	1.32	1.9
K_2O	0.43	0.47	0.49	0.49	0.56	0.53
Cr_2O_3	0.08	0.08	0.02	0.02	0.03	0.02
TiO_2	1.26	1.23	2.29	2.29	0.9	0.97
MnO	0.19	0.19	0.25	0.25	0.21	0.2
P_2O_5	0.45	0.44	0.31	0.31	0.09	0.09
SrO	0.07	0.07	0.03	0.03	0.03	0.02
BaO	0.03	0.03	0.02	0.01	0.02	0.02
LOI	0.86	1.02	0.26	0.2	1.35	1.23
Total	98.56	100.07	99.6	98.77	98.7	99.13
ppm						
Co	56	54	41	39	40	46
Ni	305	339	32	33	73	73
Pb	2	5	6	6	4	3
Sc	41	42	36	35	32	35
Zn	110	105	138	135	79	83
Ba	289	289	141.5	135.5	244	145.5
Ce	98.8	104.5	41.4	39.8	14.8	12.1
Cr	560	640	120	110	210	180
Cs	0.21	0.39	0.21	0.16	4.74	2.82
Dy	5.73	6.06	9.47	9.06	4.14	4.15
Er	2.6	2.73	5.91	5.5	2.74	2.52
Eu	3.32	3.37	2.25	2.13	1.17	1.02
Gd	9.21	10.1	8.6	8.35	4.11	3.49
Hf	3.8	3.8	5.5	5.1	2.2	1.8
Ho	1.04	1.08	2	1.93	0.93	0.85
La	39	40.9	18.1	17.6	6.5	4.7
Lu	0.29	0.32	0.79	0.8	0.42	0.38
Nb	5.7	5.6	12.1	11.6	6.5	2.1
Nd	61.1	65.2	26.9	25.8	9.9	8.7
Pr	13.8	14.45	5.83	5.65	2.06	1.75
Rb	4.1	7.1	5.7	5.5	27.6	17.3
Sm	11.7	12.75	7.1	6.93	3.07	2.59
Sr	631	610	272	251	310	232
Ta	0.2	0.2	0.7	0.7	1.3	0.1
Tb	1.15	1.17	1.52	1.33	0.68	0.63
Th	1.75	2.31	2.07	1.95	0.63	0.49
Tm	0.33	0.34	0.79	0.8	0.39	0.38
U	0.55	0.67	0.56	0.54	1.45	0.2
V	222	240	279	262	250	276
Y	25.8	27.8	52.4	50.9	24.4	23
Yb	1.92	2.24	5.37	5.21	2.74	2.52
Zr	146	146	203	199	66	60

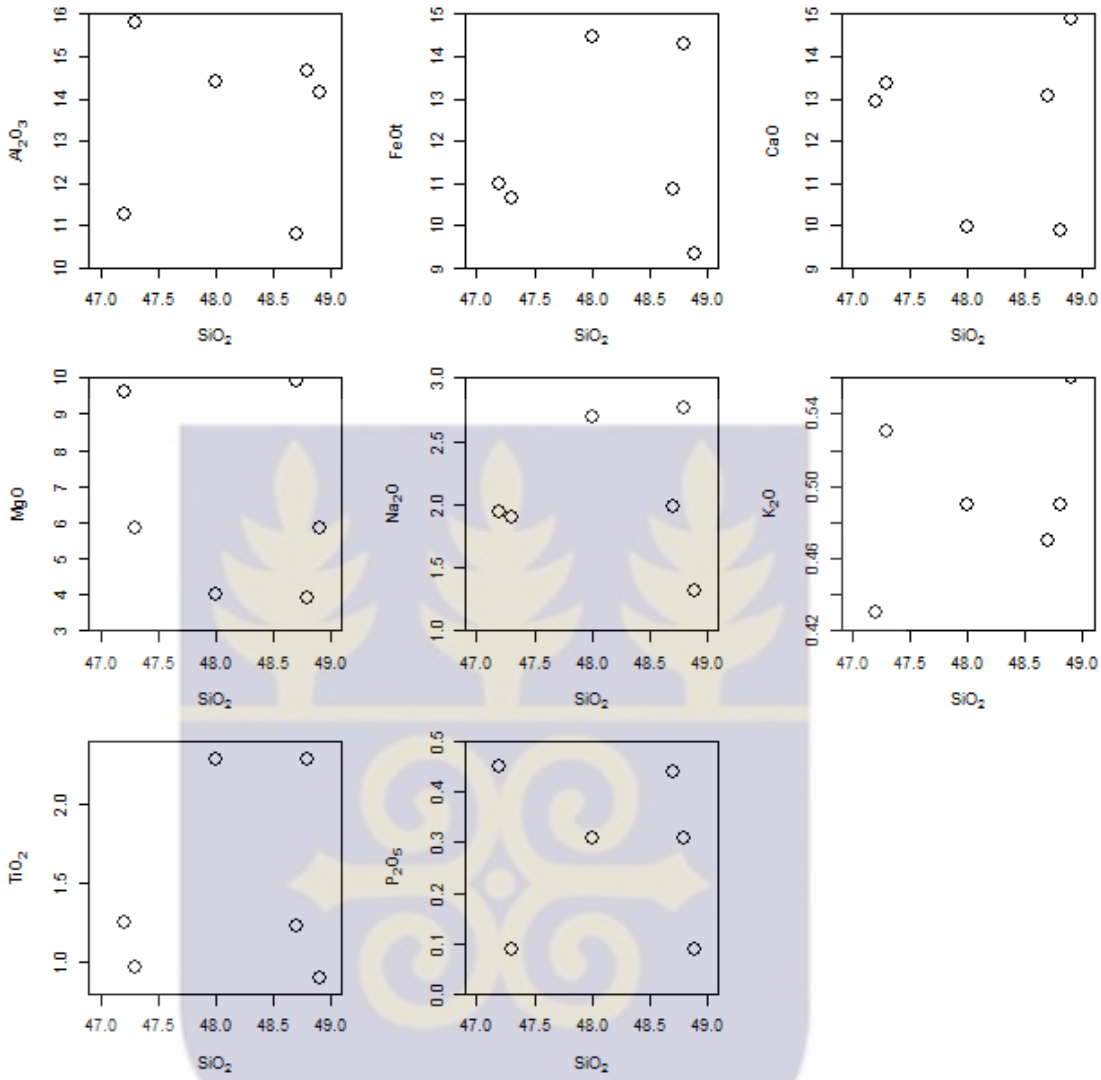

Fig. 4.10. Selected major element–SiO2 plots for the amphibolites from the study area.

4.3.2 Trace element geochemistry

The REE, transition and other significant trace element concentrations for the schists and amphibolites in the study area are presented in Tables 4.2a and b.

4.3.2.1 Schists

The REE concentrations in the schists were normalized against those of chondrites (Boynton, 1984) (Figures 4.11a, c and e). The rocks are generally more enriched in the REEs compared to the chondrites. Comparatively, the schists from the study area are more enriched in the LREEs (La_N/Sm_N = 1.43-4.13) than the HREEs (Gd_N/Lu_N = 1.31-4.03). All, except the biotite schists, show slightly negative Eu anomalies (Eu/Eu* = 0.63-0.94).

From Figure 4.11.a, the hornblende-biotite schists except sample AS01B, are two folds more enriched than the chondrites, but exhibit enrichments in the LREEs with flat patterns in the HREEs. On the whole, the hornblende-biotite schists show slightly negative Eu anomalies (Eu/Eu*=0.69-0.80), except sample AS05B which has an inconspicuous Eu anomaly.

The biotite schists are more enriched in the REEs than the chondrites but generally exhibit flattened peaks Figure 4.11.c. Sample AS09B shows an inconspicuous Eu anomaly (Eu/Eu*=0.99) whereas sample AS01A shows a slightly positive Eu anomaly (Eu/Eu*=1.02). The muscovite-biotite schists (Figure 4.11.e) are more enriched in the LREEs than in the HREEs and show slightly negative Eu anomalies (Eu/Eu*= 0.63 and 0.85).

The rare earth element (REE) concentrations in the schists from the study area were normalized against those of Post-Archean average Australian sedimentary rock; PAAS (McLennan, 1989) (Figures 4.11b, d and f).

In the diagrams, all but one hornblende-biotite schist (AS01B), were more enriched in the all the REEs than the PAAS. But sample AS05B (hornblende-biotite schist) showed a strong depletion in the HREEs with respect to PAAS. The biotite schists are more depleted in the LREEs than PAAS; whereas the muscovite-biotite schists showed flatter peaks with respect to the LREEs relative to PAAS with HREEs showing depletions relative to the PAAS.

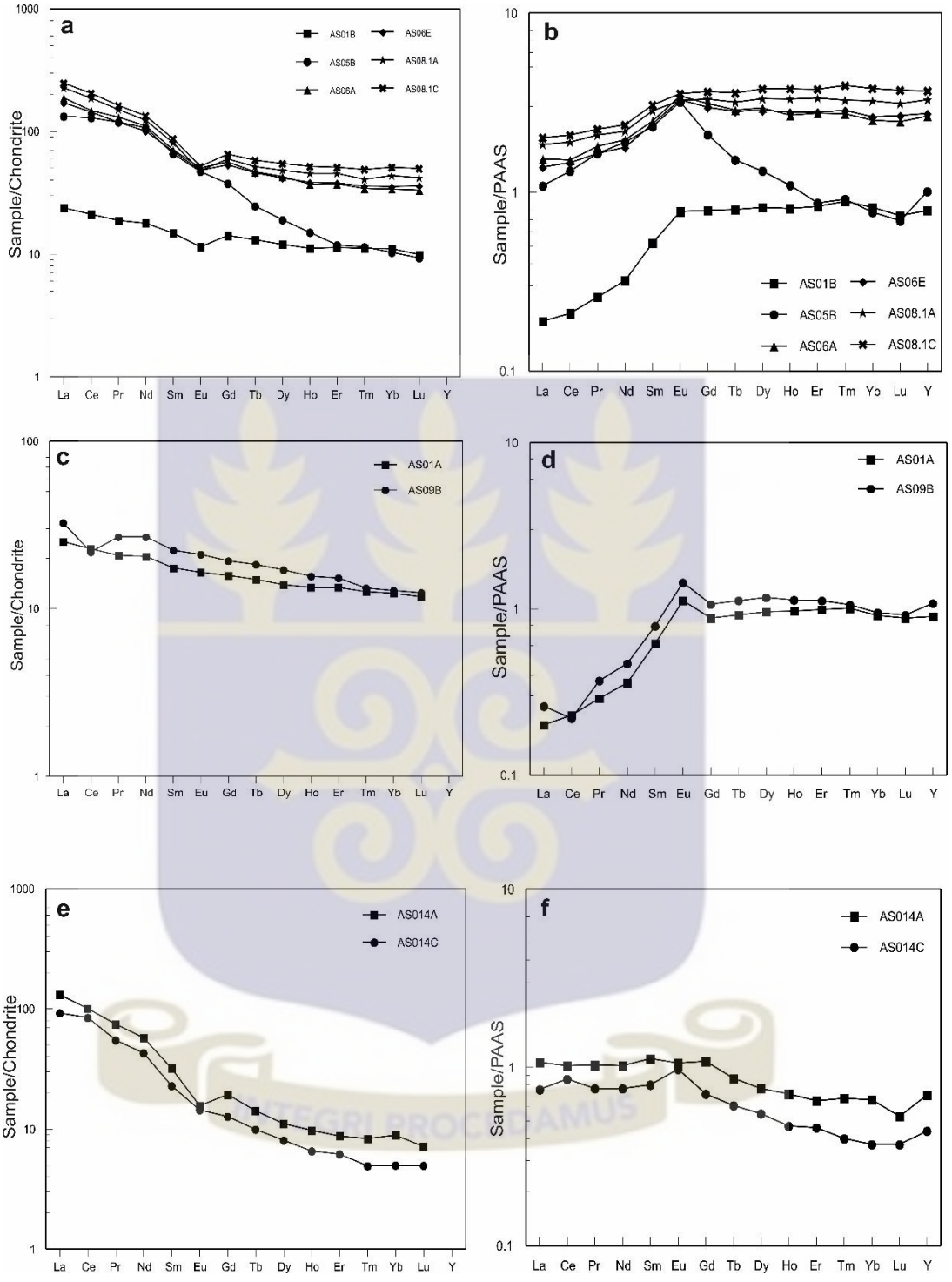

Figure 4.11. REE concentrations in individual schists from the study area normalized against REE concentrations in chondrites (average chondrite values after Boynton (1984) and REE concentrations in Post-Archean average Australian sedimentary rock PAAS (values after McLennan, 1989).

4.3.2.2. Amphibolite

The rare earth element (REE) concentrations in the amphibolites from the study area were also normalized against those of chondrites (Boynton, 1984) (Figure 4.12. a). The rocks were generally more enriched in the REEs compared to the chondrites with slight enrichments in the LREE (La_N/Sm_N = 1.14-2.09) and depletions in the HREE (Gd_N/Lu_N =3.94-3.92).

Samples AS05A and AS05C tend to be more depleted in the HREEs compared to N-MORB and E-MORB and more depleted in the LREEs compared to OIB. Samples AS015A (18) and AS015B (18) are more enriched in the HREEs than the OIB, N- and E- MORBs.

The individual amphibolites show varying Eu anomalies from slightly negative to slightly positive Eu anomalies. Samples AS05A, AS05C, AS015A (18) and AS015B (18) showed slightly negative Eu anomalies (Eu*/Eu= 0.86-0.98); whereas samples GR014A and GR014B showed slightly positive Eu anomalies (Eu*/Eu=1.01-1.04). This is an indication of the possible different types of source rocks involved in the formation of these rocks; and which helps to decipher between para- and ortho-amphibolites.

Samples AS05A, AS05C, AS015A (18) and AS015B (18) also showed strong positive peaks for terbium (Tb), while GR014A and GR014B show slightly negative peaks for Tb which tends to have a very strong correlation with thorium (Th), uranium (U) and the REEs.

Multi-element concentrations of the amphibolites were normalized against those of the Primitive Mantle (Fig. 4.12.b) to make comparisons between the incompatible trace elements and the REEs. The REEs, zirconium (Zr), yttrium (Y) and titanium (Ti) are generally considered to be immobile during metamorphism with respect to major-rock forming minerals (Ludden and Thompson, 1979; Grauch, 1989).

Strontium (Sr) in this diagram, was used as a comparison with Eu contents as a ratio used to examine the sample patterns. Samples GR014A and GR014B which showed slightly positive Eu anomalies also showed positive Sr peaks. Generally, most of the amphibolites are more enriched in most of the elements with respect to the N-MORB.

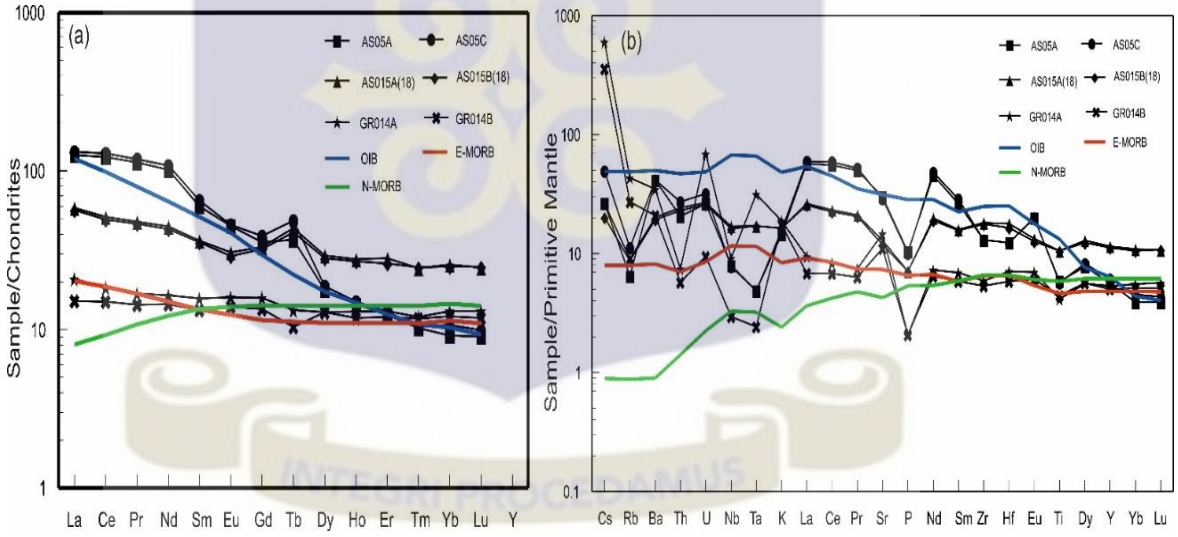

Figure 4.12.a. REE concentrations in the amphibolites from the study area normalized against REE concentrations in chondrites (average chondrite values after Boynton (1984). (b) Multi-element concentrations of the amphibolites normalized against multi-element concentrations of the Primitive mantle (average OIB, NMORB, EMORB values after Sun and McDonough (1989).

CHAPTER FIVE

DISCUSSION

5.1 SCHISTS

The results obtained from the petrographical and geochemical analysis suggest that six of the schists from the Paleoproterozoic Suhum basin are metasedimentary in nature; these are the hornblende-biotite schists (AS06A, AS06E, AS08.1C and AS08.1A) and the muscovite-biotite schists (AS014A and AS014C). The mineralogical and chemical compositions give evidence that these rocks were formed from sediments derived possibly from the erosion of mafic, intermediate and felsic igneous rocks. The relatively fine grain sizes of the minerals as well as the heterogeneity (seen as non-uniform grain sizes and orientations) are also evidence of their metasedimentary nature.

The use of geochemistry in deducing the provenance and tectonic setting of metasedimentary rocks is significant especially if the whole rock compositions of such rocks have not been significantly altered. From the Pearson correlation coefficient calculations shown in Table 4.3, the major and some selected trace element concentrations show relatively strong correlations, an indication that these rocks have undergone little or no alteration. The provenance analysis performed on these rocks would yield significantly accurate results.

The petrographical and geochemical properties of the schists from the study area have therefore been compiled and studied in order to make conclusive statements concerning the source rock types, source area weathering conditions, provenance and tectonic settings. The various elemental ratios used in this analysis are shown below.

Table 5.1. Showing some elemental ratios of the schists used in the analysis.

	Hornblende-biotite schists			Muscovite-Biotite schists		
	AS06A	**AS06E**	**AS08.1A**	**AS08.1C**	**AS014A**	**AS014C**
Al_2O_3/ SiO_2	0.25	0.25	0.21	0.21	0.23	0.19
SiO_2/Al_2O_3	4.01	3.99	4.82	4.66	4.26	5.20
K_2O/Na_2O	0.49	0.35	0.79	0.64	0.76	0.49
$Log(SiO_2/Al_2O_3)$	0.60	0.60	0.68	0.67	0.63	0.72
$log(Fe_2O_3/K_2O)$	1.04	1.17	0.70	0.75	0.25	0.42
$log(Na_2O/K_2O)$	0.31	0.46	0.10	0.19	0.12	0.31
CIA	53.29	52.25	57.29	55.25	72.00	70.64
CIW	47.56	45.79	52.03	49.37	63.37	58.00
PIA	44.70	43.72	46.78	45.12	58.34	54.06
LOI	0.35	0.26	0.33	0.26	1.23	0.62
Th/Sc	0.23	0.23	0.48	0.56	0.79	0.62
Zr/Sc	13.07	13.79	28.75	34.16	19.33	20.22
Th/U	3.88	3.75	3.74	3.78	3.14	2.92
Sm/Nd	0.21	0.22	0.21	0.21	0.18	0.17
K/Rb	0.02	0.03	0.02	0.03	0.02	0.01
Eu/Eu*	0.80	0.79	0.69	0.69	0.63	0.85
La_N/Sm_N	2.66	2.48	2.80	2.83	4.13	4.06
Gd_N/Yb_N	1.66	1.51	1.37	1.28	2.18	2.55
Ce/Ce*	0.75	0.79	0.80	0.80	0.80	0.94

5.1.1. Source weathering

The degree of source rock weathering can be measured using the Chemical Index of Alteration (CIA)= [Al_2O_3 / (Al_2O_3 +CaO* + Na_2O + K_2O) *100] by Nesbitt and Young (1982). This reveals the extent to which primary minerals (e.g. feldspars) have been transformed into aluminous clays depleted in Ca, Na and K relative to the unweathered source materials.

According to Roddaz et al. (2012), unaltered plagioclase and K-feldspars must have CIA values approximately equal to 50 as in the unaltered upper crustal rocks. The CIA values (Table 5.1) of the samples from the Suhum basin ranged between 32.49 and 72.00 (an average CIA value of 51.12). This is slightly higher than the unaltered feldspar value of 50, hence an indication of incipient to intermediate degrees of source area weathering (Roddaz et al., 2012).

The biotite schists (AS01A and AS09B) and two hornblende-biotite schists (AS01B and AS05B) exhibited no alteration as they plotted below the "feldspar join" line (Figure 5.1.a). This characteristic feature is similar to that observed in the petrography, as few of the minerals such as the feldspars exhibited low degrees of sericitization and the original pseudomorphs of these mineral grains were still clearly observed. The four schists samples; AS01A, AS01B, AS05B and AS09B, exhibited characteristics closest to those of rocks from igneous (basaltic) precursors, hence, were not used in the provenance analysis.

On the A–CN–K ternary weathering diagram by Nesbitt and Young (1984, 1989) (Figure 5.1.a), the studied samples trend parallel to the Al_2O_3-($CaO+Na_2O$) line, as the samples plot in between both Al_2O_3 and ($CaO+Na_2O$) apices, away from the CN-apex towards the A-apex and from the unaltered fields through to the "intermediate weathering intensity' fields.

Another way of evaluating the degree of weathering of source rocks is by identifying the Chemical Index of Weathering (CIW). The CIW is also a measure of the extent of conversion of feldspars to clays (Nesbitt and Young, 1984, Nesbitt and Young, 1989, Fedo et al., 1995 and Maynard et al., 1995). CIW values higher than CIA values often indicate the occurrence of K-metasomatism. The rocks from the study area have lower CIW values (Table 5.1) ranging from 30.07-63.37 (mean value of 45.43) relatively lower than the CIA values. Hence, the occurrence of K-metasomatism is not likely within the schists from the Suhum basin.

The role of source area weathering can also be assessed using the related Plagioclase Index of Alteration (PIA)= [(Al_2O_3 - K_2O) / Al_2O_3 + CaO* + Na_2O- K_2O] *100, which quantifies the degree of destruction of plagioclase and can identify albitization (Fedo et al. 1995, 1997a). Like the CIA values, PIA values around 50 are those of unweathered plagioclase and PIA values close to 100 indicate complete conversion into secondary aluminous clay minerals such as kaolinite, illite and gibbsite (Fedo et al., 1995). However, the schists from the study area showed very low PIA values (Table 5.1) ranging from 29.06- 58.34 (average PIA= 42.59); away from the C-apex towards the A-K apex. This confirms the results from the CIA (Figure 5.1.b).

And again the results from the petrographical studies, indicates the presence of whole plagioclase feldspars (unaltered) as well as those undergoing minimal levels of weathering with their original pseudomorphs still visible in thin sections. Figure 5.1.b below also indicates that the schists have varying feldspar contents from andesine; also confirmed in thin section. As plagioclase feldspars with twinning closer in similarity to the above mentioned minerals, than typical albites.

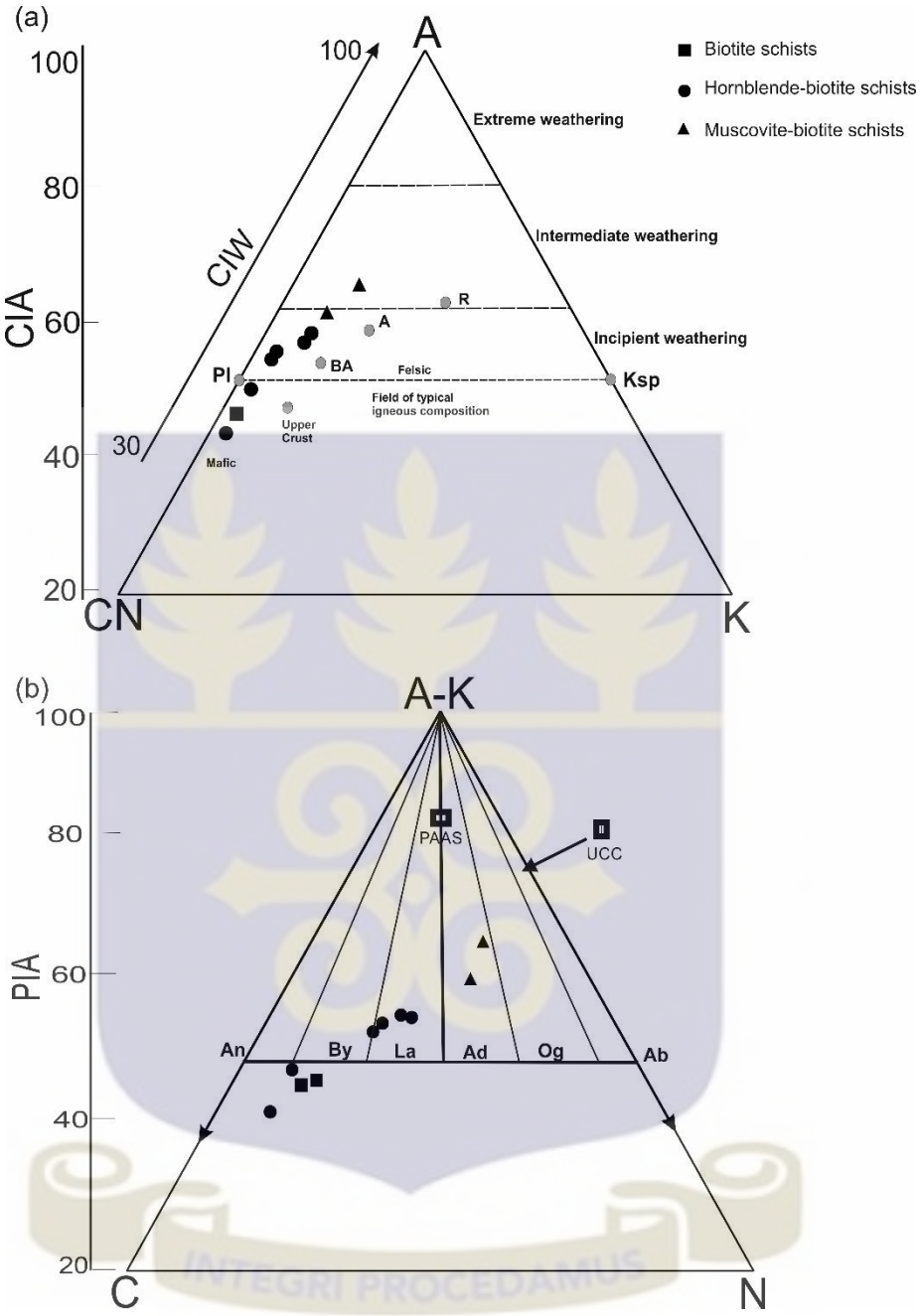

Figure 5.1. (a) A–CN–K ternary weathering diagram; Nesbitt and Young, 1984, 1989. A=Al2O3; CN = CaO*+Na2O; K = K2O. CIA, Chemical Index of Alteration. Mineral compositions: Pl, plagioclase; Ksp, K-feldspar; after Nesbitt and Young (1984). UCC, upper continental crust; PAAS, post-Archean Australian shale (Taylor and McLennan, 1985). (b) Ternary weathering diagram; AK–C–N ternary plot (after Fedo et al., 1997). A–K = Al2O3–K2O; C = CaO*; N = Na2O; (molar proportions). PIA, Plagioclase Index of Alteration; An, anorthite; By, bytownite; La, labradorite; Ad, andesine; Og, oligoclase; Ab, albite.

According to McLennan and Taylor (1991), Th/U ratios also give an indication of source area weathering. Environments with reducing conditions tend be have reconcentrations of U during sedimentation, which lowers the Th/U ratios. Therefore, Th/U ratios greater than 3 usually reflect weathering effects. The provenance type can also be deduced from this ratio, Th/U ratios less than 3 may be interpreted in terms of provenance.

Sediments derived from active margins have Th/U ratios ranging from 1 to 6, and low Th contents (McLennan et al., 1993). And Th/U ratios below 3.5–4.0 (typical of upper crust igneous rocks) are common in post-Archean turbidites but absent in their Archean counterparts (McLennan and Taylor, 1991). These ratios are also typically high (4–7) in PAAS. From the study, the Th/U ratios (Table 5.1) of the schists, however, range from 2.63-4.37 (average value of 3.49) with very low Th values of 0.42-10.7 ppm (averaged 4.96). The weathering trends of the schists gradually progress from very low to moderate with respect to the Th/U ratios of the PAAS as they tend to plot above the depleted mantle arc sources as shown in Figure 5.2.

The LOI values coupled with the low Chemical Index of Alteration (CIA) and Plagioclase Index of Alteration (PIA) values, positive correlation of the High Field Strength Elements (HFSEs), as well as the minimal amounts of visible partial or secondary replacement of minerals from the petrographical analysis, are all indications that the schists have undergone little or no alteration.

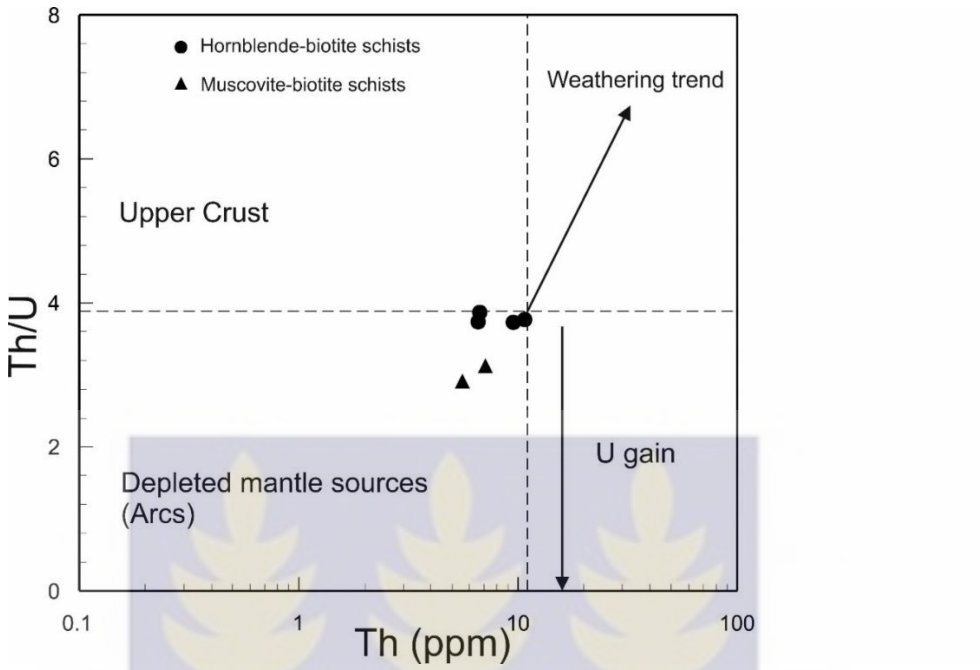

Figure 5.2. Th–Th/U plot for the studied samples. Dashed lines: Th/U ratio and Th content of UCC; fields for depleted mantle sources from McLennan et al. (1993). Arrows indicate direction of trends for weathering (U loss) and enrichment (U gain).

5.1.2 Classification

The classification of the schists as well as the maturation determinants are clearly seen in the petrographical studies as the mineralogical compositions are made up mostly of ferromagnesian minerals (least resistant) which have undergone little or no sediment reworking with the sediments clearly showing heterogeneity (a sign of textural immaturity).

Figure 5.3.a, shows the geochemical classification of Herron (1988). Most of the studied samples (hornblende-biotite schists) enriched in Fe_2O_3 plot in the iron-rich shale field and two samples (hornblende-biotite schists and muscovite-biotite schists) fall in the wacke field and close to the intersection between the Fe-Shale, shale, Fe-sand and wacke fields.

This shows that the schists tend to exhibit a sandy nature than shales, and the petrography reveals that the rocks display a predominantly granular texture. The classification diagram by Pettijohn et al. (1972) (Figure 5.3.b) also confirms low to moderate degrees of sediment maturation in these rocks which plot within the greywackes field. A closer observation of the classification diagram by Herron (1988) shows majority of the samples shifting closer to the Fe-sand boundary, emphasizing the immatured sandy nature of the sediments which make up these rocks as confirmed by Pettijohn et al., (1972) (Figure 5.3.a).

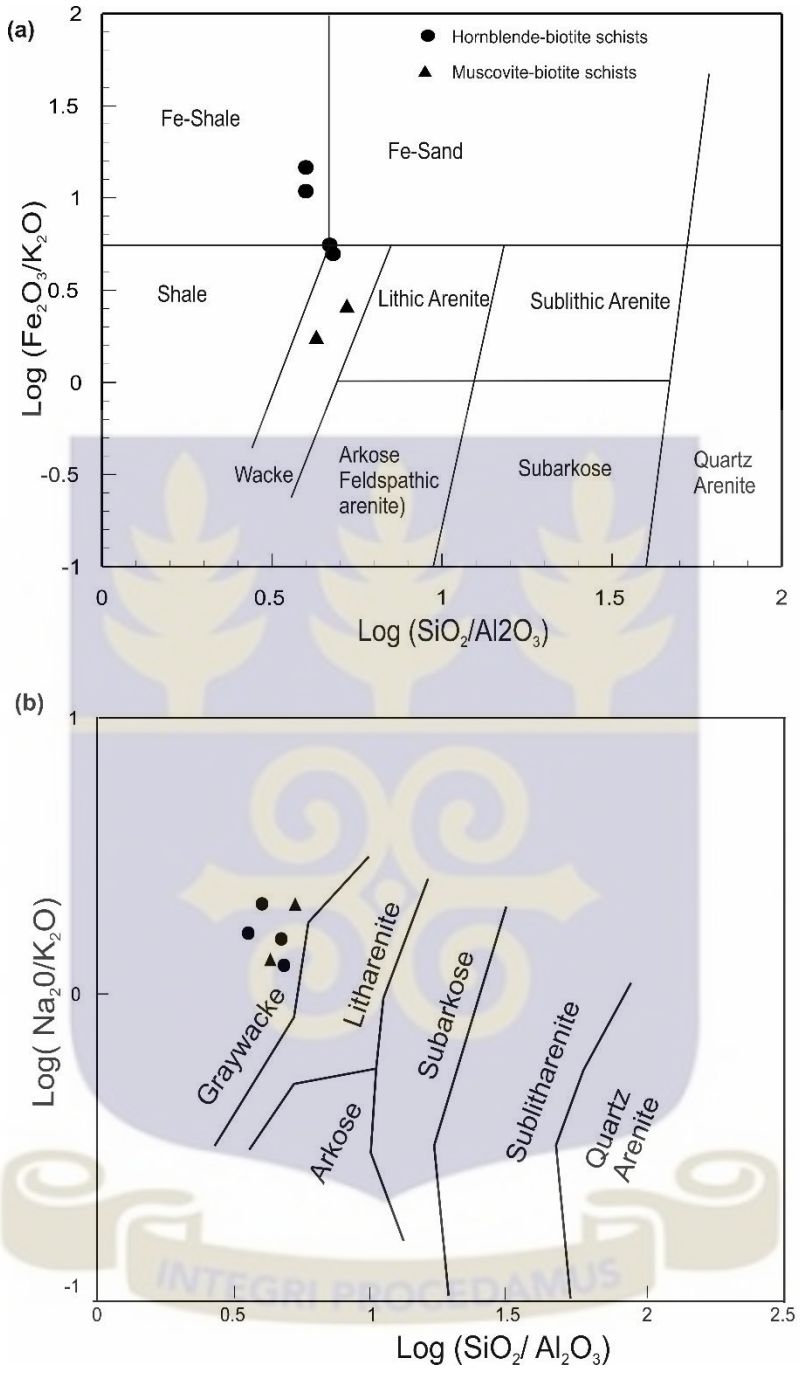

Figure 5.3. (a) Geochemical classification and compositional maturity diagram (Herron, 1988) showing the relatively low to moderate degrees of maturation of these schists. (b) The geochemical classification of the schists from the study area using log (Na_2O/K_2O) vs log (SiO_2/Al_2O_3) from Pettijohn et al. (1972) with boundaries redrawn by Herron (1988).

5.1.3 Sediment maturation

The SiO_2/Al_2O_3 ratios of the schists in the study area are relatively low (3.51-5.20), indicating low degrees of sediment maturation (Fig 5.2). The studied samples also show low to moderate degrees of sediment maturation in the Silica-Alkali-Mafic (SAM) plot (Fig. 5.4); the progression in the degree of maturation is highest within the muscovite-biotite schists relative to the other rocks confirmed by the high percentages of SiO_2 (67.7-71.3 wt%) and high quartz contents (35-45%) as well. The plot also shows that these rocks were possibly derived from rhyolitic (felsic) magma sources as a cluster of the plots is observed around the rhyolitic field.

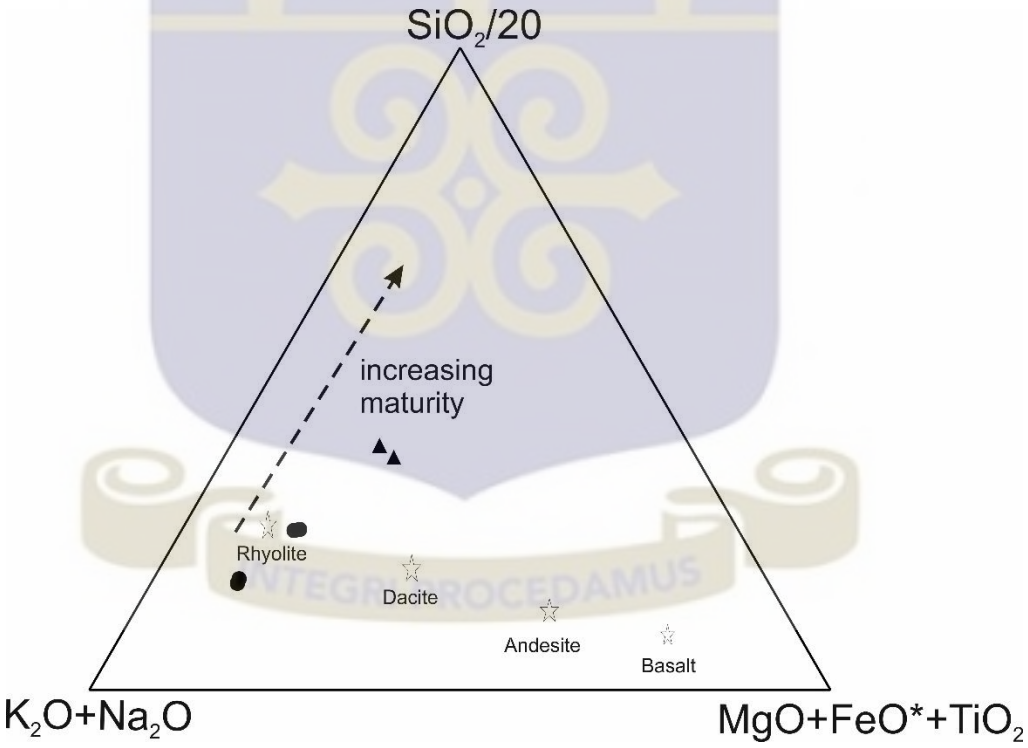

Figure 5.4. SAM plot showing the primary igneous compositional trend between basalt and rhyolite (Roser and Korsch 1999). The muscovite-biotite schists are almost displaced towards the SiO2 apex, consistent with increase of quartz through recycling, with the rest of the schistose rocks displaced closer to K-N apex.

The degree of sediment maturity (sediment recycling) can also be shown by the Zr/Sc values (Table 5.1) ranging from 1.64-34.16. The Th/Sc-Zr/Sc diagram in Figure 5.5.b shows that the rocks have undergone little or no sediment recycling whatsoever. As the samples plot within the mantle field where little or no sediment recycling usually occurs; in the mantle region there is no addition of zircons as the occurrence of magma evolution does not occur much.

Therefore, the metasedimentary rocks from the study area within the Suhum Paleoproterozoic basin were probably formed from sediments which have undergone little or no sediment reworking or recycling and are immature both texturally and mineralogically. Hence, the sediments are relatively close to the source region and have not been transported far from their sources.

5.1.4 Source rock composition

According to petrographical data obtained, several ratios and plots have been used to define the source rocks of the schists. Sc and Th often tend to be transferred easily from source rocks to sediment, hence, Th/Sc ratios reflect bulk source compositions (Taylor and McLennan, 1985; McLennan and Taylor, 1991). In first-cycle sediments, Th/Sc ratios show an overall positive correlation with Zr/Sc, depending on the nature of the source rock, whereas Zr/Sc ratios in mature or recycled sediments display considerable variation with little accompanying change in Th/Sc (McLennan et al., 1993).

A plot of the Th/Sc versus Zr/Sc (Figure 5.5b) shows most the analysed schists exhibiting a positive correlation within the mantle compositional fields with the low Th/Sc values. This is a reflection of the dominant input of rock materials from the mantle region having varying mineral or elemental compositions, with no clear contribution from the Upper continental crust. A plot of Th versus Sc adopted from McLennan et al. (1993) in Figure 5.5c, shows the analyzed samples exhibiting a wide variety of source rock compositions from mafic through to intermediate to felsic sources with minimal continental signatures.

Figure 5.5 shows the K–Rb relationships by Floyd et al, (1990) indicating that most of the data fall in the acid to intermediate magmatic precursor. The relatively high K_2O values also confirm that these rocks were possibly derived from areas of acidic to intermediate chemical compositions.

The high percentages of highly unstable minerals as compared to stable minerals, is an indication of a more mafic source input and evident that these rocks occurred within a possible arc tectonic setting such as a volcanic arc. The presence of minerals which are less resistant to weathering processes is also an indication that these rocks are in close proximity to their source rocks and have undergone little or no weathering or alteration. Mineralogical maturity is also low within these rocks.

Therefore, the rocks from the study area within the Suhum Paleoproterozoic basin are metasedimentary rocks formed from the sedimentation of rock materials from mafic through to intermediate and felsic rock sources. This deduction supports the geology of the Birimian metavolcanic rocks being the probable source; as they comprise of basaltic and basaltic andesitic, as well as, granitic rocks.

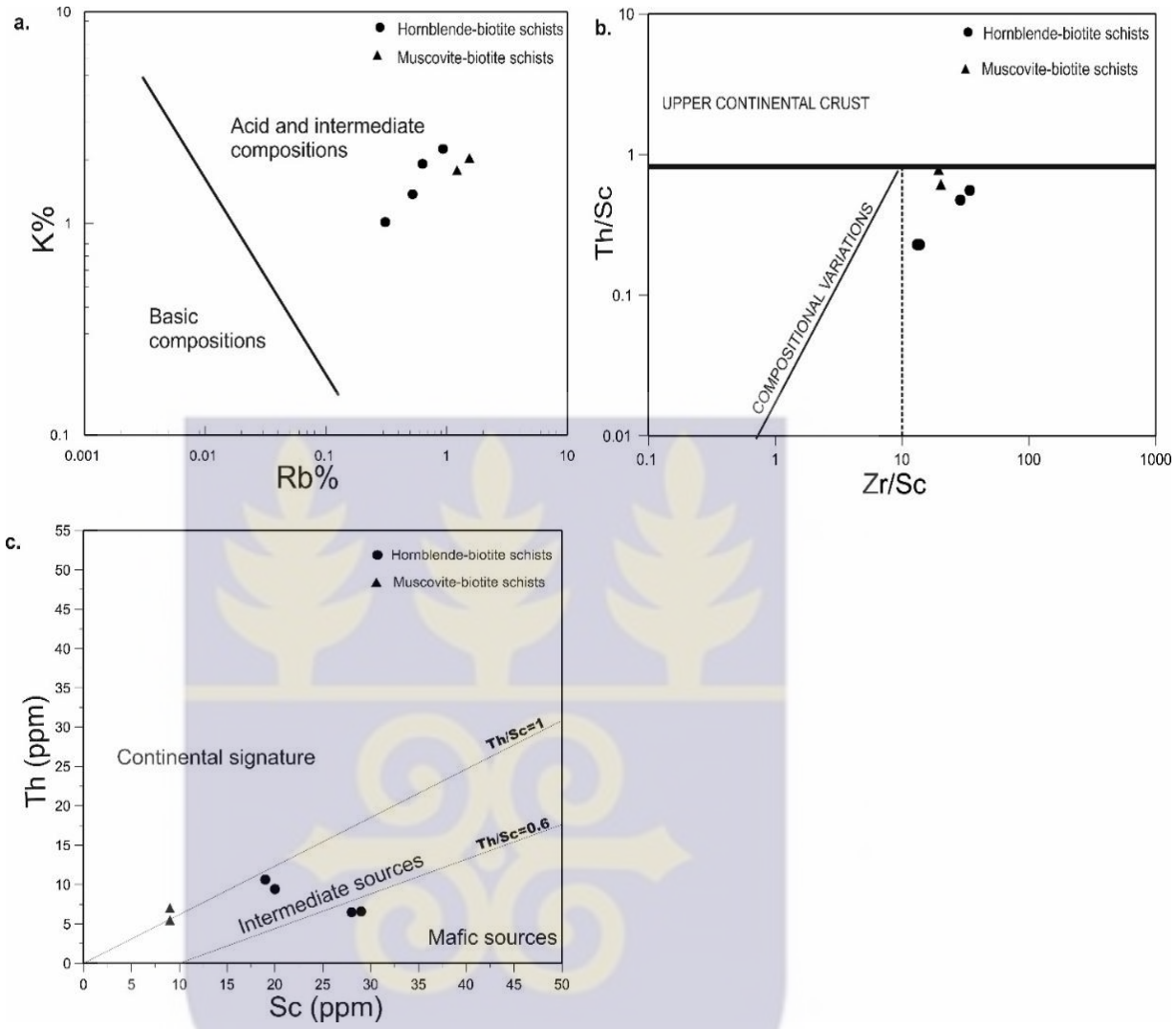

Figure 5.5. (a) Plot for the discrimination of source rocks of the studied samples; K vs. Rb (Floyd et al., 1990). (b) Th/Sc vs. Zr/Sc provenance and recycling discrimination plot (after McLennan et al., 1990). The data cluster within the mantle compositional field and show no enrichment of Zr (commonly employed to indicate sediment recycling). Th/Sc<1 reflects provenance of samples from the mantle (McLennan, 2001). Relatively low Zr/Sc ratios (<40) in these samples suggest low to moderate degrees of recycling. (c) Th versus Sc plot, adopted from McLennan et al. (1993) showing the source areas of the schists from the study area.

5.1.5. Provenance

McLennan et al. (1993, 1995) described five major provenance types on the basis of geochemistry, the characteristics of which are summarized in Table 5.2. From this study, majority of the results obtained suggest that the sources of the schists from the study area within the Suhum Basin are typical of Young Undifferentiated Arc terranes. The evidence leading to this conclusion are;

1. Unevolved major and trace element compositions (e.g., low SiO_2/Al_2O_3, Th/Sc, Zr/Sc ratios) presented in Table 5.1,
2. Variations of major and trace element compositions in Table 4.2a, low negative Eu anomalies, and
3. Low REE abundances, and variable but less LREE enrichment when compared with those of Early Proterozoic Crust (EPC) and Post Archean Australian Sedimentary rock (PAAS).

From the provenance discriminatory diagram (Fig. 5.8.) after Roser and Korsch (1988), the schists from the study area exhibit signatures of metasedimentary rocks made up of sediments derived from igneous sources as these rocks plot within igneous provenance fields (mafic, intermediate and felsic). The elemental ratios, La/Sc, La/Cr, La/Co, Th/Sc, Th/Cr and Th/Co are particularly critical of provenance (Cullers and Podkovyrov, 2000). Compared to the ratios of the early Proterozoic volcanic rocks of different compositions, the analyzed schists show varying La/Sc, Th/Sc, La/Cr, La/Co, Th/Cr, Th/Co ratios similar to each of the early Proterozoic volcanic rocks (Table 5.3).

The hornblende-biotite schists (AS06A, AS06E, AS08.1A and AS08.1C) and muscovite-biotite schists (AS014A and AS014C) exhibit ratios similar to early Proterozoic felsic volcanic rocks.

REE patterns have been used widely in geochemical studies of metasedimentary rocks. The degree of differentiation of LREE from HREE is a measure of the proportion of felsic to mafic components in the source region, whereas Eu anomalies may provide information about the nature of the processes affecting the source area, such as whether plagioclase has been removed from the ultimate igneous source areas of the sediments (Taylor and McLennan, 1985). The LREE enrichment of the analyzed samples is relatively less (La_N/Yb_N; average mean value =2.6) as compared to that of PAAS and EPC (La_N/ Yb_N = 4.3 and 3.9 respectively according to Condie, 1993). This suggests the dominance of mafic rocks over felsic rocks in the source areas, the slightly negative Eu-anomalies for most of the schists is also an indication of the dominance of felsic and andesitic rocks within the source region (Taylor and McLennan, 1985).

From the La - Th - Sc ternary plot with fields defined by Girty and Barber (1993) shown in Figure 5.7, the studied rock samples, exhibit magmatic-arc and oceanic island alkali basalt-related signatures. It can also be observed that these rocks show wide variations in the source rock compositions from andesites, felsic volcanic rocks and early Proterozoic greywackes.

Table 5.2. Summary of geochemical characteristics of provenance types (after McLennan et al., 1993, 1995).

Terrane type	Eu/Eu*	Th/Sc	Other geochemical features	Description
Old Upper Continental Crust (OUC)	~0.60-0.70	~1.0	Evolved major element compositions (e.g. High Si/Al, CIA); High LILE abundances, uniform compositions.	Old igneous/metamorphic/ sedimentary terranes affected intracrustal differentiation. Stable cratons, old foundation of active settings.
Recycled Sedimentary Rocks (RSR)	~0.60-0.70	≥1.0	Evidence of heavy mineral concentrations in trace elements (e.g. Zr, Hf for Zircon, REE for monazite).	Recycled sedimentary/ metasedimentary rocks specifically identified. If not separately identified part of OUC.
Young Undifferentiated Volcanic Arc (YUA)	~1.0	<1.0	Unevolved major element compositions (e.g. Low Si/Al, CIA); High LILE abundances, variable compositions.	Young mantle-derived volcanic/ plutonic arc rocks. Dominates forearcs, component in continental arcs, backarcs.
Young Differentiated Volcanic Arc (YUA)	~0.50-0.90	Variable	Evolved major element compositions (e.g. High Si/Al, CIA); High LILE abundances, variable compositions.	Young mantle-derived volcanic/ plutonic arc rocks affected by intracrustal differentiation. Similar environments as YUA but more mature arcs or more dissection.
Various exotic components: Chemical signature depends on the nature of the component. For example, very high Mg, Cr, Ni, V and Cr/V would be distinctive of ophiolitic sources.				

Table 5.3 A comparison of provenance elemental ratios of the Birimian schists from the study area within the Suhum Basin and the early Proterozoic volcanic rocks (Condie, 1993 in Asiedu et al., 2004).

	Suhum Schists							Felsic volcanics	Andesites	Basalts
	AS06A	**AS06E**	**AS08.1A**	**AS08.1C**	**AS014A**	**AS014C**				
							Mean	**Mean**	**Mean**	**Mean**
La/Sc	2.01	1.89	3.52	4.03	4.53	3.19	**2.08**	**1.88**	**1.05**	**0.32**
La/Cr	1.94	2.65	3.52	3.83	0.82	0.41	**1.34**	**3**	**0.31**	**0.08**
La/Co	3.07	2.78	7.81	10.94	3.14	2.87	**3.19**	**5**	**0.74**	**0.29**
Th/Sc	0.23	0.23	0.48	0.56	0.79	0.62	**0.30**	**0.5**	**0.17**	**0.07**
Th/Cr	0.22	0.33	0.48	0.54	0.14	0.08	**0.18**	**0.8**	**0.05**	**0.02**
Th/Co	0.35	0.35	1.06	1.53	0.55	0.56	**0.45**	**1.33**	**0.12**	**0.06**

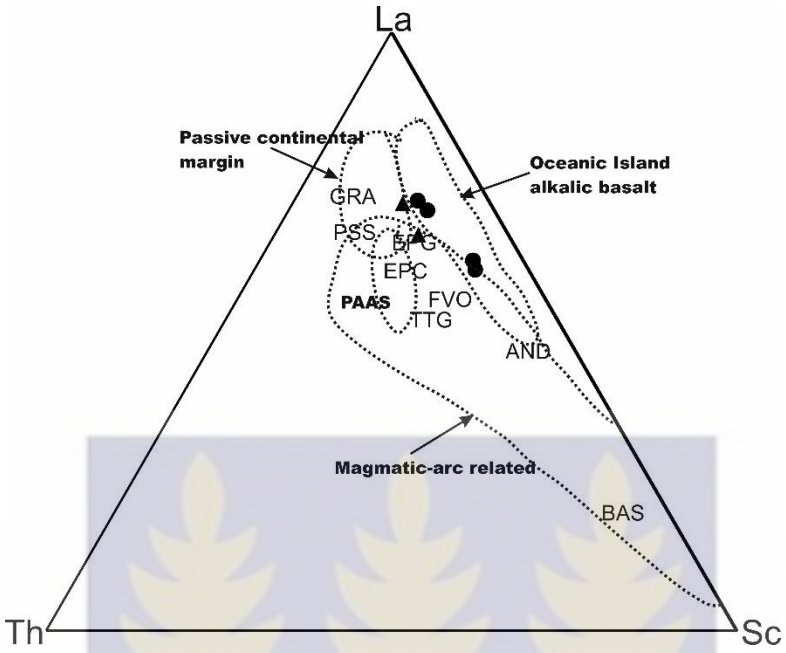

Figure 5.7. La - Th - Sc ternary plot with fields defined by Girty and Barber (1993). Source rock compositions (volcanics) are of early Proterozoic age (Condie, 1993). BAS = basalts; AND = andesites; FVO = felsic volcanic rocks; TTG = Proterozoic tonalite-trondjhemite-granodiorite; EPC = early Proterozoic crust; EPG = early Proterozoic graywackes; PSS = Proterozoic sandstones; GRA = Proterozoic granites (Condie, 1993).

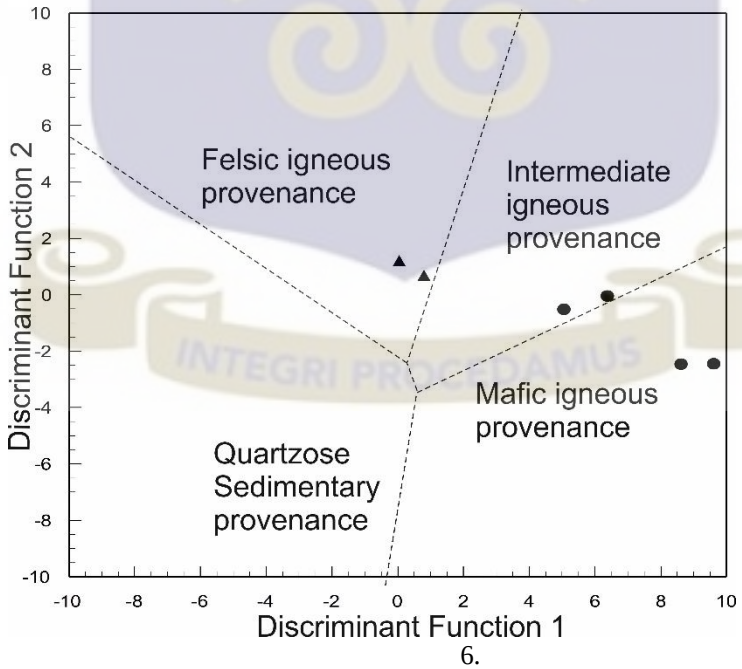

6.

Figure 5.8. Discriminant function diagram for the provenance signatures of the schists from the Paleoproterozoic Suhum basin using major elements (after Roser and Korsch, 1988).

6.1.6. Tectonic Settings

The composition of sediments is controlled by the composition of its source rocks, which in turn is controlled by the tectonic setting of these sources. It is therefore possible to classify clastic sediments on the basis of tectonic environment of their source terrain.

According to Crook (1974), greywackes which are quartz-rich (> 65% quartz) are associated with passive continental margins. Quartz-poor greywackes (< 15%) are associated with magmatic island arcs and greywackes with intermediate quartz (15-65% quartz) are indicative of an active continental margins. From Table 4.1a, the schists (which initially showed characteristics of greywackes in Figure 5.3b) have quartz compositions ranging from (10-45) %, average quartz composition of 31.7%, representing felsic to intermediate quartz composition and revealing both magmatic island arcs and active continental margin setting for these rocks.

Maynard et al. (1982) stated that major element geochemistry has been employed largely to decipher ancient tectonic settings. On SiO_2-K_2O/Na_2O, Al_2O_3/SiO_2-Fe_2O_3+ MgO and SiO_2 / Al_2O_3-K_2O/Na_2O diagrams (by Maynard et al., 1982; Bhatia, 1983 and Roser and Korsch, 1986) (Figure 5.6.), the studied samples show considerable range of compositions, hence, interpretations of the tectonic setting using these compositions are not straightforward. Na and K are among the most mobile major elements, and the use of Na_2O and K_2O to discriminate tectonic settings may be regarded cautiously.

The SiO_2 and K_2O/Na_2O values increase from volcanic arc, to active continental margin to passive margins. For the studied samples, the plot of K_2O/Na_2O versus SiO_2 by Roser and Korsch (1988), indicate that the schists are typical of modern sediments from volcanic arc and active continental margins.

According to studies conducted by Roser and Korsch (1988), volcanic arc and active continental margin sediments are generally quartz-poor sediments in accordance with low SiO_2 contents (Figure 5.6b). Unstable minerals (less resistant minerals) such as the pyroxenes, hornblendes and biotites usually exist within active margins and arc tectonic settings; when preservation occurs before alteration occurs. The hornblende-biotite schists from the study area, exhibit characteristics of rocks from more active tectonic settings, evident in the high mineralogical compositions of these unstable minerals.

From the discrimination diagram (after Bhatia, 1983) based on the bivariate plot of Al_2O_3/SiO_2 vs (Fe_2O_3 + MgO), the analyzed samples plot mostly within oceanic, continental and active continental arc margins (Figure 5.6c). The tectonic setting discrimination diagram (Roser and Korsch, 1988) based on major element compositions of studied rock samples using SiO_2/Al_2O_3 vs. K_2O/Na_2O, also indicate that the metasedimentary rock samples were deposited within active continental margin and arc margins and further categorizes arc margin type based on the detritus components within these rocks; A1-basaltic, and andesitic detritus arc setting, A2-felsitic–plutonic detritus evolved arc setting (Figure 5.6a).

Therefore, the schists from the study area within the Suhum Basin occur within an active continental margin, as well as, continental and oceanic arc settings with basaltic, andesitic and felsic-plutonic detritus components. These deductions support the geology from already existing literature concerning the tectonic settings in which the Birimian Paleoproterozoic rocks occur.

The Birimian Paleoproterozoic rocks formed during the Eburnean event; which is seen as an accretionary orogeny resulting from the collision of island arcs and oceanic plateau with an Archean craton. The Birimian terrane is an accretionary environment, where the rock-forming materials are all accreted to form the rocks, typical of an active continental margin. Some researchers such as Ama-Salah (1996) and Vidal and Alric (1994), proposed the involvement of subduction processes in the generation of the Paleoproterozoic Birimian terranes, hence the rocks would give off arc signatures.

According to the literature, sedimentation and volcanism occur contemporaneously. Hence, both active continental signatures and arc signatures should the most be conclusive results to be obtained. The A1 and A2 settings also support the geology of the probable source region of the rocks from the study area, been the Birimian metavolcanics.

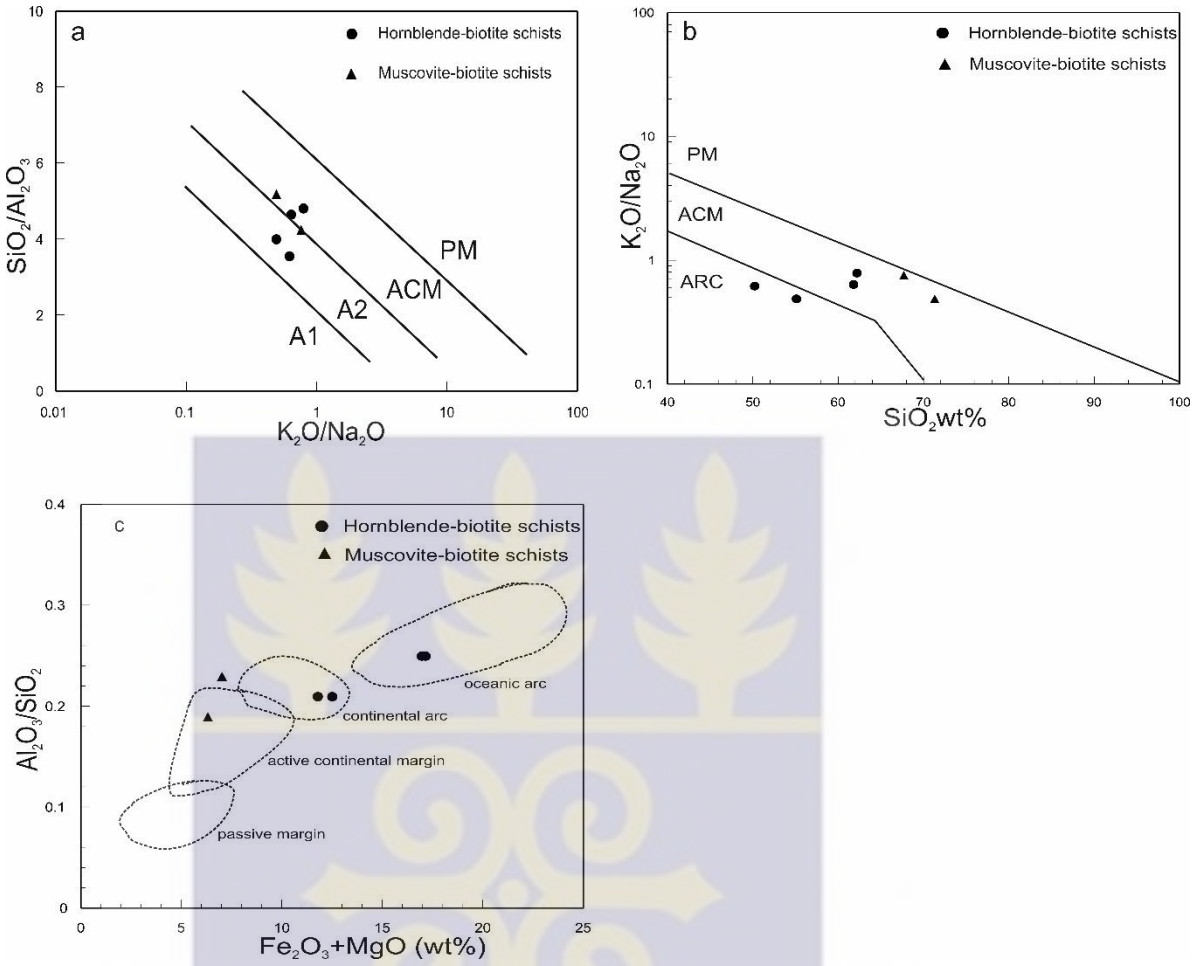

Figure 5.6. (a) Tectonic setting discrimination (Roser and Korsch, 1988) diagram based on major element compositions of studied rock samples. SiO2/Al2O3 vs. K2O/Na2O (Maynard et al., 1982; Roser and Korsch, 1986; Gu et al., 2002). ACM, active continental margin; PM, passive margin; A1, arc setting, basaltic, and andesitic detritus; A2, evolved arc setting, felsitic–plutonic detritus. (b) Tectonic setting discrimination (Roser and Korsch, 1988) diagram based on major element compositions of studied rock samples. ACM, active continental margin; PM, passive margin; ARC, oceanic island arc. (c) Discrimination diagram for the metasedimentary rocks (after Bhatia, 1983) based on bivariate plot of Al_2O_3/SiO_2 vs (Fe_2O_3 + MgO).

5.1.7. Comparison with metasedimentary rocks from other Birimian metasedimentary basins of known provenance and tectonic settings in Ghana.

Comparatively, more research has been done on the rocks from other Birimian metasedimentary basins than those of the Suhum basin. Hence, to gain a better understanding of the rocks from the Suhum basin, data from other studies conducted on metagraywackes from the Cape coast basin (Asiedu et al., 2004) and the Kumasi basin (Asiedu et al., 2009) was studied in order to make conclusive comparisons with respect to the provenance, tectonic settings, paleoweathering conditions and source rock compositions.

The studies on the rocks from both Kumasi and Cape Coast basins (Asiedu et al., 2004, 2009) yielded quite similar results to that of the current study. Both researches identified that these rocks were derived from localized sources of mixed felsic, intermediate, mafic and TTG granites possibly from the adjacent Birimian granite-greenstone belts. These rocks were all believed to have been deposited in active tectonic settings similar to modern island arcs (oceanic and continental) with minimal involvement from the older upper crust. All evidences suggest that these rock sources are representative of Young Undifferentiated Arc (YUA) Terranes.

5.2 AMPHIBOLITES

The geochemical data were plotted on various discriminatory diagrams to establish the evolution of the amphibolites. An attempt was made to identify whether these rocks are ortho-amphibolites (derived from igneous rocks) or para-amphibolites (derived from sedimentary sources). For successful discrimination between the two amphibolite types several criteria can be used.

5.2.1 Classification

The SiO_2 versus $Na_2O + K_2O$ plot of Cox et al. (1979) (Figure 5.9a) suggests the gabbroic, basic and subalkaline (tholeiitic) nature of these amphibolites. The gabbroic as well as subalkaline or tholeiitic character of these rocks is also confirmed on the petrogenetic plot of Miyashiro (1974), which is typical of Precambrian mafic volcanism (Engel et al., 1965) and the AFM ternary plots by Irvine and Baragar (1971) as shown in Figures 5.9c and 5.9d respectively. The concentrations of the stable oxide Al_2O_3 in the samples are relatively high and hence are classified as metaluminous rocks according to the classification scheme of Kuno (1960) having mean values of 13.51 wt% (Figure 5.9b).

In deciphering between para-amphibolites and ortho-amphibolites, the use of the rare earth element concentrations is very significant. Amphibolites with mafic igneous rock precursors tend to not show negative Eu anomalies in their REE patterns; whereas, amphibolites whose precursor is a post-Archean greywacke or shale show negative Eu anomalies.

From the analysis and spider diagrams (Figure 4.13a) on the amphibolites from the study area, samples AS05A, AS05C, ASO15A (18) and AS015B (B) show slightly negative Eu anomalies (Eu*/Eu= 0.86-0.98) while the remaining samples GR014A and GR014B, showed slightly positive Eu anomalies(Eu*/Eu=1.01-1.04).

Also, high concentrations of elements such as barium (Ba) and strontium (Sr) in amphibolites are usually not in accordance with ortho-amphibolites. This is observed within samples AS05A, AS05C, AS015A (18) and AS015B (18); confirming the fact these amphibolites are para-amphibolites.

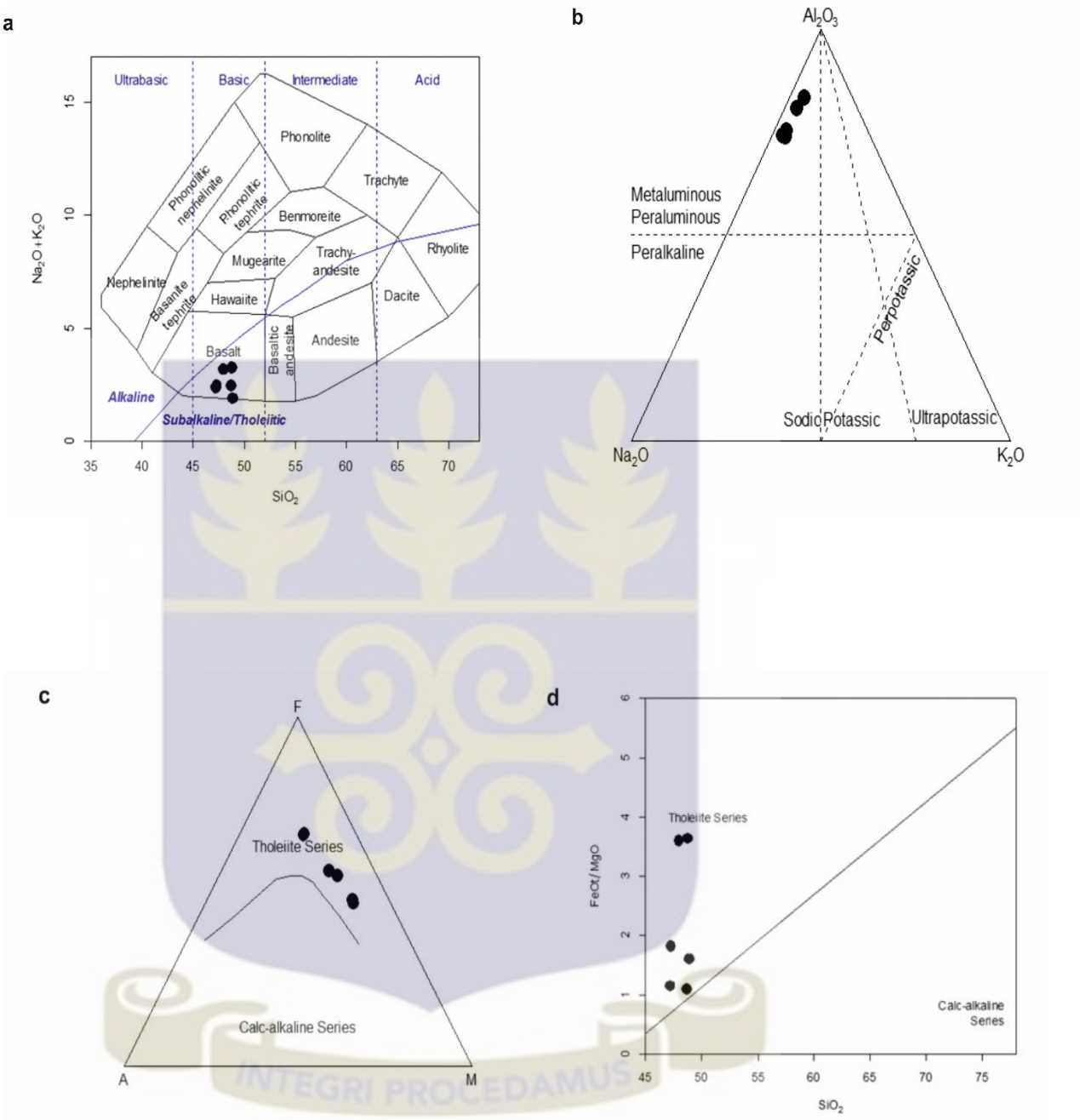

Figure. 5.9 (a). Total alkali (Na_2O+K_2O) versus SiO_2 discrimination diagram of Cox et al (1979), showing the gabbroic and subalkaline/tholeiitic nature of the amphibolites from the study area. (b) Al_2O_3 – K_2O – Na_2O Ternary diagram (Kuno, 1960), also classifying the metaluminous nature of the amphibolites from the study area. c. The AFM ternary diagram by Irvine and Baragar (1971), showing the tholeiitic nature of the amphibolites from the study area. d. FeOt/MgO versus SiO_2 discrimination diagram (after Miyashiro, 1974), also showing the tholeiitic affinity of the amphibolites from the study area.

5.2.2 Tectonic settings

The amphibolites from the study area plotted within the Oceanic and Continental Island arc settings as shown in Figure 5.2.10a. This was also confirmed by the $10MnO\text{-}TiO_2\text{-}10P_2O_5$ tectonic setting discriminatory plots (Figure 5.10b) showing the samples plotting within the island arc tholeiitic (IAT), continental arc basaltic(CAB) settings and Mid-Ocean ridge basaltic(MORB) setting boundaries. Using the geotectonic setting discriminatory plots by Verma et al (2006) in Figure 5.11., the samples mostly plot within all the tectonic fields in all five (5) diagrams, but are dominant within the Mid-Ocean Ridges, Island Arc, Oceanic island arc settings.

The use of immobile trace and minor elements to determine the petrogenesis and tectonic settings of volcanic or plutonic rocks is widespread (Smith and Smith, 1976; Winchester and Floyd, 1977; Pearce and Norry, 1979). According to Glikson (1971), metavolcanic or metaplutonic rocks of Archean calc-alkaline volcanic series are more differentiated and have lower K, Ba, Sr and Zr values higher than those of metabasalts of ultrabasic and basic assemblages and recent oceanic tholeiites. The concentrations of the trace elements of the schists are similar to values obtained for Low-K volcanic suites, and with those obtained from primitive Precambrian tholeiites. The abundances of the compatible elements Ni (mean 137.5 ppm) and Cr (mean 303 ppm) in the amphibolites are also typical of Archean tholeiites (Gill, 1979).

Further trace element characterisation can be achieved using the Zr/Y versus Zr diagram (Figure 5.10a) of Pearce and Norry (1979), which shows that the amphibolite samples fall within the Within-plate basalt field, with mixed signatures within the Mid-Ocean ridge and island-arc basalt fields.

Large Ion Lithophile trace elements (LILE), K, Rb, Cs, Ba, Pb and Sr which are incompatible (except for Sr and Ba in plagioclase) tend to be enriched in the Oceanic Island Basalts (OIB) with respect to Mid-Ocean Ridge Basalt (MORB). In most of the amphibolites from the study area; K, Cs, Ba and Sr tend to be more enriched in these (showing positive peaks) elements, an indication that these rocks were possibly derived as a result of oceanic intraplate volcanism.

Therefore, the amphibolites from the study area were probably derived from subduction zones and exhibit signatures typical of Mid-Ocean ridge basaltic rocks, island arc tholeiitic basalts and continental arc basalts. These support the fact that Paleoproterozoic terranes of the West African Craton resemble the Archean greenstone terranes. The Archean domain of the West African craton is made up of extensive granite-gneiss complexes are locally associated amphibolites and metasedimentary rocks.

The Birimian Paleoproterozoic rocks formed during the Eburnean event; where the accretionary orogeny resulting in collisions of island arcs and oceanic plateau with an Archean craton. Hence, these amphibolites were probably derived from the metamorphism of the Birimian rocks within the Suhum basin.

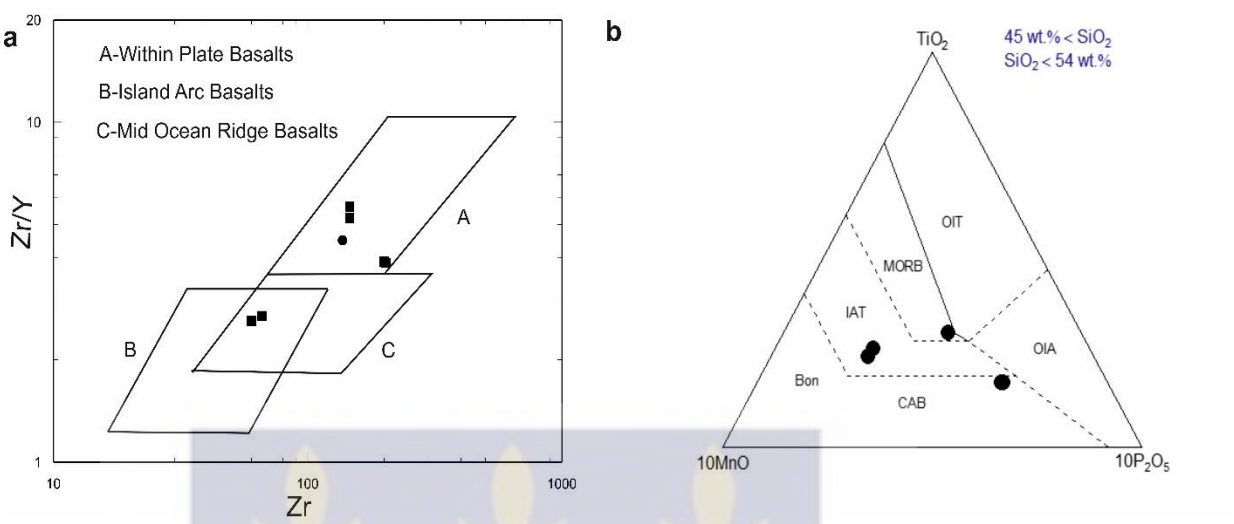

Figure 5.10. a. Discrimination diagram, after Pearce and Norry et al (1979) showing the Within Plate Basalts, the mix of Island Arc and Mid-Ocean Ridge Basalts. b. A tectonic setting discrimination diagram, after Mullen (1983).

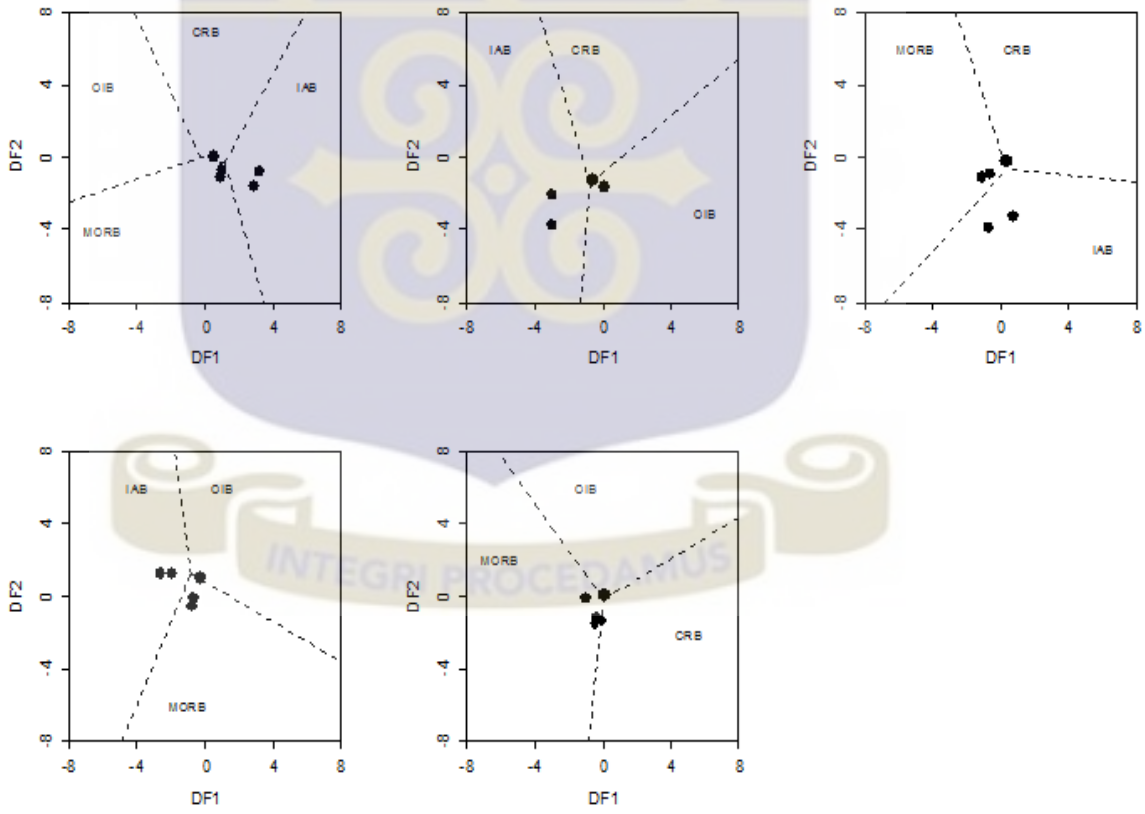

Figure 5.11. Geotectonic setting discrimination diagrams for basic and ultrabasic rocks, after Verma et al. (2006) IAB: Island Arc Basalts; MORB: Mid-Ocean Ridge Basalts; CRB: continental rift basalts and OIB: Oceanic Island Basalts.

CHAPTER SIX

CONCLUSIONS AND RECOMMENDATIONS

6.1. CONCLUSIONS

The schists and amphibolites from the Suhum basin have been thoroughly studied using petrography and geochemistry. The main focus of this study was on rocks such as the hornblende-biotite schists, muscovite-biotite schists and amphibolites (because the other rocks were not concerned as being metasedimentary in nature). From this study, the following conclusions have been made.

6.1.1. Schists

The schists observed within the study area include biotite schists, hornblende-biotite schists and muscovite-biotite schists, but more emphasis was placed on the hornblende-biotite schists and muscovite-biotite schists; which are categorized as metasedimentary rocks. These two types of schists are geochemically classified as iron-rich shales (Fe-shales) and wackes; and generally as greywackes. The schists have undergone incipient to intermediate degrees of weathering and were derived from unweathered to slightly weathered source rocks.

The source rocks of these schists may have experienced low to intermediate degrees of sediment recycling and have not been transported far from their sources. Petrographical and geochemical analysis of the rocks suggest low degrees of alteration and little or no sediment recycling. The schists are both texturally and mineralogically immature, and they were most likely derived from deeper crustal and upper mantle sources exhibiting

compositional variations from felsic, intermediate and mafic magmatic sources with little or no contribution from the upper continental crust.

The inferred provenance and source rocks imply that these rocks are most likely derived from the adjacent Birimian volcanic belts. The schists were derived from andesites, felsic volcanic rocks and early Proterozoic greywackes, with variable source rock compositions. The sources of these rocks were most likely deposited within active continental margin and arc margin settings. The general provenance suggests that the schists are typical of Young Undifferentiated Arc terranes within felsic, intermediate and mafic igneous provenances.

The characteristics of the schists from the study area appear similar to that of metasedimentary rocks within the Kumasi and Cape Coast Basins.

6.1.2. Amphibolites

The amphibolites from the study area were classified as metaluminous, gabbroic and subalkaline (tholeiitic) in nature. Four of these amphibolites are classified as para-amphibolites and two are ortho-amphibolites. These rocks were probably derived from subduction zones characteristic of Mid-Ocean Ridge Basalts (MORBs), Island Arc Tholeiites (IATs) and Continental Arc Basalts (CABs). Supporting the fact that Paleoproterozoic terranes of the West African Craton resemble the Archean greenstone terranes. In conclusion, the amphibolites were most probably derived from the adjacent Birimian granite-greenstone belts and show characteristics similar to the Archean greenstone belts.

6.1. RECOMMENDATIONS

The Birimian Paleoproterozoic Suhum basin generally lacks extensive studies, hence this work is deficient in the input of all the various aspects of the earth sciences especially with respect to geology. It is therefore highly recommended that extensive and detailed geological field mapping be undertaken within areas of the Basin to gain a better understanding of the various rock types, structures as well as, field relationships.

Regardless of the limitations to this research, the findings are consistent. Further work should be considered to aid in a proper reconciliation of the petrogenesis, provenance and tectonic settings of the Birimian rocks within the Basin.

REFERENCES

Abouchami, W., Boher, M., Michard, A. and Albarede, F. (1990). A major 2.1 Ga old event of mafic magmatism in West Africa: An early stage of crustal accretion. Journal of Geophysical Research, 95: 17605–17629.

Alric, G. (1990). Geochemistry of Birimian volcanism (Lower Proterozoic of the Haute-Comoe Unite, Northeastern Ivory Coast –Preliminary results. Journal of African Earth Science, 10 (4): 669-681.

Ama Salah, I., Liégeois, J.P., Pouclet, A. (1996). Evolution of an early Birimian oceanic island arc of the Nigerian Liptako (Sirba): geology, geochronology and geochemistry. Journal African Earth Science, 22 (3): 235–254.

Anum, S., Asamoah Sakyi P., Su B., Nude P.M., Nyame F., Asiedu D., Kwayisi D. (2015). Geochemistry and geochronology of granitoids in the Kibi-Asamankese area of the Kibi-Winneba volcanic belt, southern Ghana, Journal of African Earth Science 102: pp.166-179.

Arndt, N.T., Naldrett, A.J., Pyke, D.R. (1977). Komatiitic and iron-rich tholeiitic lavas of Munro township, Northeast Ontario. Journal of Petrology. 18, 319–369.

Asiedu, D.K., Dampare, S.B., Asamoah Sakyi, P., Banoeng-Yakubo, B., Osae, S., Nyarko, B.J.B., Manu, J., (2004). Geochemistry of Paleoproterozoic metasedimentary rocks from the Birim diamondiferous field, southern Ghana: implications for provenance and crustal evolution at the Archean-Proterozoic boundary. Geochemical Journal, 38: 215–228.

Asiedu, D. K., Kutu, J. M., Manu, J., Hayford, E. K. (2009). Geochemistry and Provenance of Metagreywackes from the Kononogo area, Southwestern Ghana. African Journal of Science Technology, 10: 37-44.

Attoh, K., Evans, M.J., Bickford, M.E. (2006). Geochemistry of an ultramafic-rodingite rock association in the Palaeoproterozoic Dixcove greenstone belt, southwestern Ghana. Journal of African Earth Science 45: 333–346.

Baratoux, L., Metelka, V., Naba, S., Jessell, M.W., Grégoire, M., Ganne, J. (2011). Juvenile Paleoproterozoic crust evolution during the Eburnean orogeny (~2.2-2.0Ga), western Burkina Faso, Precambrian Research, 191 (1), 18-45.

Bhatia, M.R. (1983). Plate tectonics and geochemical composition of sandstones. Journal of Geology 92, 181–193.

Black, R., Liégeois, J.P. (1993). Cratons, mobile belts, alkaline rocks and the continental lithospheric mantle: The Pan-African testimony. Journal of Geological Society, London, 150: pp. 89-98.

Boher, M., Abouchami, W., Michard, A., Albarede, F. and Arndt, N. T. (1992). Crustal growth in West Africa at 2.1 Ga. Journal of Geophysical Research. 95: 345–369.

Boynton, W.V. (1984). Cosmochemistry or the rare earth elements: meteorite studies. In: Henderson, P. (Ed.), Rare Earth Element Geochemistry. Elsevier, Amsterdam, pp. 63–114.

Condie, K. C. (1993). Chemical composition and evolution of the upper continental crust: Contrasting results from surface samples and shales. Chemical Geology, 104: 1–37.

Cox, K. G., Bell, J. D., and Pankhurst, R. J. (1979). The interpretation of igneous rocks: London, George Allen & Unwin, 450 p.

Crook, K.A.W. (1974). Lithogenesis and geotectonics: the significance of compositional variations in flysch arenites (graywackes). In: R.H. Dott and R.H. Shaver (Editors), Modern and Ancient Geosynclinal Sedimentation. Society of Economic and Paleontological Mineral Special Publications, 19: 304-310.

Cullers, R. L. and Podkovyrov, V. N. (2000) Geochemistry of the Mesoproterozoic Lakhanda shales in southeastern Yakutia, Russia: implications for mineralogical and provenance control, and recycling. Precambrian Research 104, 77–93.

Davis, D. W., Hirdes, W., Schaltegger, U. and Nunoo, E. A. (1994) U-Pb age constraints on deposition and provenance of Birimian and gold-bearing Tarkwaian sediments in Ghana, West Africa. Precambrian Research 67: 89–107.

Delor, C., Lafon, J.M., Lahondére, D., Roever, E.D., Fraga, M.L., Rossi, P. (2001). Palaeoproterozoic framework of the Guiana Shield II-continental scale boudinage and ultra-high temperature granulite belt exhumation at 2.07-2.06 Ga. Simpósio de Geologia da Amazonia, 7.

Dickson, K.B., Benneh, G. (1988). A New. Geography of Ghana. Longmans.

Eisenlohr, B., Hirdes, W. (1992). The structural development of the early Proterozoic Birimian and Tarkwaian rocks of southwest Ghana, West Africa. Journal of African Earth Science 14: 313–325.

Engel, A.E.J., Engel, C.G. and Havens, R.G. (1965). Chemical characteristics of oceanic basalts and the upper mantle. Geological Society, American Bulletin. 76: pp. 719-734.

Ennih, N., Liégeois, J. P. (2008). The boundaries of the West African craton, with special reference to the basement of the Moroccan metacratonic Anti-Atlas belt. Geological Society, London, Special Publications, 297: 1-17.

Fedo, C.M., Nesbitt, H.W. and Young, G.M. (1995). Unraveling the effects of potassium metasomatism in sedimentary rocks and paleosols, with implications for paleoweathering conditions and provenance. Geology 23, 921–924.

Fedo C.M., Young G.M., Nesbitt H.W. (1997a). Paleoclimatic control on the composition of the Paleoproterozoic Serpent Formation, Huronian Supergroup, Canada: Harbinger of continental glaciation Precambrian Research 86, Issues 3–4, 22: 201-223.

Feybesse, J.L., Billa, M., Guerrot, C., Duguey, E., Lescuyer, J.L., Milési, J.P., Bouchot, V. (2006). The Paleoproterozoic Ghanaian province: geodynamic model and ore controls, including regional stress modelling. Precambrian Research 149: 149–196.

Floyd, P.A., Franke, W., Shail, R., Dörr, W. (1990). Provenance and depositional environment of Thenohercynian synorogenic greywacke from the Giessen nappe, Germany. Geologische Rundschau 79, 611–626.

Ganne J., De Andrade V., Weinberg, R.F., Weinberg, R.F., Vidal O., Dubacq B., Kagambega N., Naba S., Baratoux, L., Jessell, M., Allibon, J. (2012). Modern-style plate subduction preserved in the Paleoproterozoic West African Craton. Nature Geoscience, 5 (1), 60-65.

Geological Survey Department (2009). Geological map of Ghana 1:1000000. Ghana Geological Survey and Bundesanstalt für Geowissenschaften und Rohstoffe. Geological Survey Department of Ghana, Accra, Ghana.

Girty, G. H. and Barber, R. W. (1993). REE, Th, and Sc evidence for the depositional setting and source rock characteristics of the Quartz Hill chert, Sierra Nevada, California. Processes Controlling the Composition of Clastic Sediments (Johnsson, M. J. and Basu, A., eds.), Geological Society, America, Special Papers 284: 109–119.

Glikson, A.Y. (1971). Primitive Archean element distribution patterns: chemical evidence and geotectonic significance. Earth Planet Science Letters 12: 309-320.

Griffis, R. J., Barning, K., Agezo, F. L., Akosah, F. K. (2002). Gold Deposits of Ghana. Accra, Ghana: Minerals Commission.

Gu, X.X., Liu, J.M., Zheng, M.H., Tang, I.X., Qi, L. (2002). Provenance and tectonic setting of the Proterozoic turbidites in Hunan, south China: geochemical evidence. Journal of Sedimentary Research 72, 393–407.

Herron, M.M. (1988). Geochemical classification of terrigenous sands and shales from core or log data. Journal of Sedimentary Petrology 58, 820–829.

Hirdes, W., Davis, D. W., Eisenlohr, B. N. (1992). Reassessment of Proterozoic granitoid ages in Ghana on the basis of U/Pb zircon and monazite dating. Precambrian Research 56: 89–96.

Hirdes, W., Davis, D.W., Lüdtke, G., Konan, G. (1996). Two generations of Birimian (Palaeoproterozoic) volcanic belts in north eastern Côte d'Ivoire (West Africa), as demonstrated by precise U–Pb mineral dating: consequences for 'Birimian controversy. Precambrian Research 80: 173–199.

Irvine, T.N., Baragar, W.R.A. (1971). A guide to chemical classification of the common volcanic rocks. Canadian Journal of Earth Sciences 8, 523–548.

Junner, N. R. (1940) Geology of the Gold Coast and Western Togoland (with revised geological map). Bulletin of Gold Coast Geological Survey 11: 40.

Junner, N. (1935). Gold in gold coast. Accra, Ghana: Geological Survey Department.

Kuno, H. (1960). High-alumina basalt. Journal of Petrology 1: 12-145.

Ledru, P., Pons, J., Milesi, J.P., Feybesse, J.L., Johan, V. (1991). Transcurrent tectonics and polycyclic evolution in the Lower Proterozoic of Senegal-Mali. Precambrian Research 50: 337–354.

Ledru, P., Milesi, J.P., Vinchon, C., Johan, V., Marcoux, E., Ankrah, P. (1988). Géologie et gîtologie de l'or des series birrimiennes du Ghana. BRGM report, 88AFO 122 GEO, p. 36.

Leube, A., Hirdes, W., Mauer, R. and Kesse, G. O. (1990). The early Proterozoic Birimian Supergroup of Ghana and some aspects of its associated gold mineralization. Precambrian Research 46: 139–165.

Liégeois, J. P., Claessens, W., Camara, D., Klerkx, J. (1991). Short-lived Eburnean orogeny in southern Mali. Geology, tectonics, U–Pb and Rb–Sr geochronology. Precambrian Research, 50: 111–136.

Lüdtke, G., Hirdes, W., Konan, G., Kone, Y., Yao, C., Diarra, S., Zamble, Z. (1998). Geologie de la région Haute Comoe Nord avec carte géologique 1/100,000. Feuilles Kong. 4B, 4d, et Tehini-Bouna 3a–3d. Bull. No. 1 DG: Abidjan, p. 178.

Maynard, J.B., Valloni, R., Yu, H. (1982). Composition of modern deep sea sands from arc-related basins. Geological Society of London, Special Publication, vol. 10, pp. 551–561.

Maynard, J.B., Morton, J., Valdes-Nodarse, E.L., Diaz-Carmona, A. (1995). Sr isotopes of bedded barites; guide to distinguishing basins with Pb-Zn mineralization. Economic Geology, 90 (7), 2058-2064.

McLennan, S. M. (1989) Rare earth elements in sedimentary rocks: Influence of provenance and sedimentary processes. Reviews in Mineralogy and Geochemistry 21: 169–200.

McLennan, S.M., Taylor, S.R., (1991). Sedimentary rocks and crustal evolution: tectonic setting and secular trends. Journal of Geology 99: 1–21.

McLennan, S. M., Hemming, S. R., McDaniel, D. K. and Hanson, G. N. (1993). Geochemical approaches to sedimentation, provenance and tectonics. Processes Controlling the Composition of Clastic Sediments (Johnsson, M. J. and Basu, A., eds.), Geological Society, America, Special Papers 284: 21–40.

McLennan, S.M., Hemming, S.R., Taylor, S.R., Eriksson, K.A. (1995). Early Proterozoic crustal evolution: Geochemical and Nd Pb isotopic evidence from metasedimentary rocks, southwestern North America", Geochimica et Cosmochimica Acta, 59 (6): 1153-1177.

McLennan, S.M. (2001). Relationships between the trace element composition of sedimentary rocks and upper continental crust. Geochemistry Geophysics Geosystems, vol. 2, paper number 2000GC000109.

Milesi, J. P., Feybesse, J. L., Ledru, P., Dommanget, A., Ouedraogo, M. F., Marcoux, E., Prost, A., Vinchon, C., Sylvain, J. P., Johan, V., Tegyey, M., Calvez, J. Y., Lagny, P. (1989). West African gold deposits. Chronique de la recherche miniere, BRGM report no. 497, 3-98.

Milesi, J.P., Ledru, P., Ankrah, P., Johan, V., Marcoux, E., Vinchon, C. (1991). The metallogenic relationship between Birimian and Tarkwaian gold deposits in Ghana. Mineralium Deposita, 26 (3), 228-238.

Milesi, J.P., Feybesse, J.L., Pinna, P., Deschamps, Y., Kampunzu, H., Muhongo, S., Lescuyer, J.L., Le Goff, E., Delor, C., Billa, M., Ralay, F. (2004). Geological map of Africa 1: 10,000,000, SIGAfrique project. In 20th Conference of African Geology, BRGM, Orléans, France (pp. 2-7).

Miyashiro, A. (1974). Volcanic rock series in island arcs and active continental margins. American Journal of Science 274, 321–355.

Moon, P.A., Mason, D. (1967). The geology of ¼ field sheets 129 and 131. Bompata SW and NW Ghana Geological Survey Bulletin 31: 1-51.

Mullen, E.D. (1983). $MnO/TiO_2/P_2O_5$: A minor element discriminant for basaltic rocks of oceanic environments and its implications for petrogenesis, Vol. 62, (1), pp. 53-62.

Nesbitt, H.W., Young, G.M. (1982) Early Proterozoic climates and plate motions inferred from major element chemistry of lutites. Nature 299: 715–717.

Nesbitt, H.W., Young, G.M. (1984) Prediction of some weathering trends of plutonic and volcanic rocks based on thermodynamic and kinetic considerations. Geochim. Cosmochim. Acta 48: 1523–1534.

Nesbitt, H.W., Young, G.M. (1989). Formation and diagenesis of weathering profiles. Journal of Geology 97: 129.

Pearce, J.A., Norry, M.J. (1979). Petrogenetic implications of Ti, Zr, Y and Nb variations in volcanic rocks. Contributions to Mineralogy and Petrology 69: 33–47.

Pettijohn, F.J., Potter, P.E., Siever, R. (1972). Sand and Sandstones. Springer – Verlag, New York, p. 618.

Pouclet, A., Vidal, M., Delor, C., Simeon, Y., Alric, G. (1996). Le volcanisme birimien du nord-est de la Côte d'Ivoire, mise en evidence de deux phases volcano-tectoniques distinctes dans l'evolution geodynamique du Paleoproterozoique. Bulletin de la Société géologique de France, 167 (4): 529-541.

Pouclet, A., Doumbia, S., Vidal, M. (2006). Geodynamic setting of the Birimian volcanism in central Ivory Coast (western Africa) and its place in the Palaeoproterozoic evolution of the Man Shield. Bulletin de la Societe Geologique de France, 177 (2): 105–121.

Rathamaro, S., Demange, M., Fonteilles, M., Joron, J.L., Treuil, M. (1988). La série birrimienne de Perkoa (Burkina-Faso). Géochimie et minéralogie. Interprétation lithostratigraphique. Conséquences sur l'interprétation géodynamique du Birrimien. Comptes rendus de l'Académie des sciences de Paris, Sér. II, 307: pp. 2033–2040.

Rosa-Costa L.T., Ricci P.S.F., Lafon J.M., Vasquez M.L., Carvalho J.M.A., Klein E.L., Macambira E.M.B. (2003). Geology and geochronology of Archean and Paleoproterozoic domains of the southeastern Amapá and northwestern Pará, Brazil-southeastern Guiana Shield. Géologie de la France, 2(3),4.

Roser, B.P., Korsch, R.J. (1986). Determination of tectonic setting of sandstone-mudstone suites using SiO2 content and K2O/Na2O ratio. Journal of Geology 94: 635–650.

Roser, B.P., Korsch, R.J. (1988). Provenance signatures of sandstone-mudstone suites determined using discriminant function analysis of major-element data. Chemical Geology 67: 119–139.

Smith, R.E., Smith, S.E. (1976). Comments on the use of Ti, Zr, Y, Sr, K, P and Nb in classification of basaltic magmas. Earth Planet. Sci. Lett. 32: 114-120.

Sun, S.S., McDonough, W.F. (1989). Chemical and isotopic systematics of oceanic basalts: implication for mantle composition and processes. In: Saunders, A.D., Norry, M.J. (Eds.), Magmatism in Ocean Basins, vol. 42. Geological Society of London Special Publication, pp. 313–345.

Sylvester, P. J., Attoh, K. (1992). Lithostratigraphy and composition of 2.1 Ga greenstone belts of the West African Craton and their bearing on crustal evolution and the Archean-Proterozoic boundary. Journal of Geology 100: 377–393.

Tagini, B. (1971). Esquisse structurale de la Côte D'Ivoire. Essai de géotectonique régionale. Thèse Univ. Lausanne. Société d'Etat pour le Développement minière de la Côte D'Ivoire.

Tagini, B. (1972). Esquisse structurale de la Côte D'Ivoire. Essai de géotectonique régionale, Vol. 5, Sodemi.

Taylor, S. R., McLennan, S. M. (1985). The Continental Crust: Its Composition and Evolution. Blackwell Scientific, Oxford.

Taylor, P. N., Moorbath, S., Leube, A. and Hirdes, W. (1992) Early Proterozoic crustal evolution in the Birimian of Ghana: constraints from geochronology and isotope geology. Precambrian Research 56: 97–111.

Thieblemont, D., Goujou, J.C., Egal, E., Cocherie, A., Delor, C., Lafon, J.M. Fanning, C.M. (2004). Archean evolution of the Leo Rise and its Eburnean reworking, Journal of African Earth Sciences, 39(3): 97-104.

Triboulet, C., Feybesse, J.L. (1998). Les métabasites birimiennes et archéennes de la région de Toulepleu-Ity (Côte D'Ivoire): des roches portées ã 8 kbar (~24km) et 14 kbar (~42 km) au Paléoprotérozoic. Comptes Rendus de l'Academie des Sciences-Series IIA-Earth and Planetary Science Letters 327 (1): 61-66.

Verma, S.P., Guevara, M., Agrawal, S. (2006). Discriminating four tectonic settings: Five new geochemical diagrams for basic and ultrabasic volcanic rocks based on log–ratio transformation of major-element data. Journal of Earth System Science 115 (5): 485–528.

Vidal, M., Alric, G., (1994). The Palaeoproterozoic (Birimian) of Haute-Comoé in the West African Craton, Ivory Coast: a transtensional back-arc basin. Precambrian Research 65: 207–229.

Villeneuve, M., Cornée, J. J. (1994). Structure, evolution and palaeogeography of the West African craton and bordering belts during the Neoproterozoic. Precambrian Research, 69, pp. 307–326.

Winchester, J., Floyd, P. (1977). Geochemical discrimination of different magma series and their differentiation products using immobile elements. Chemical Geology 20: 325– 343.